NATIONAL ADVISORY COMMITTEE FOR AERONAUTICS

TECHNICAL NOTE 4326

LIGHTNING HAZARDS TO AIRCRAFT FUEL TANKS

By J. D. Robb, E. L. Hill, M. M. Newman, and J. R. Stahmann

Lightning and Transients Research Institute

Washington

September 1958

NATIONAL ADVISORY COMMITTEE FOR AERONAUTICS

TECHNICAL NOTE 4326

LIGHTNING HAZARDS TO AIRCRAFT FUEL TANKS

By J. D. Robb, E. L. Hill, M. M. Newman, and J. R. Stahmann

SUMMARY

The hazards of lightning strokes to aircraft fuel tanks have been investigated in artificial-lightning-generation facilities specifically constructed to duplicate closely the natural lightning discharges to aircraft determined through flight research programs and analysis of lightning-damaged aircraft over a period of many years. Explosion studies were made in an environmental explosion chamber using small fuel tanks under various simulated flight conditions.

The results showed that there is a primary hazard whenever there is direct puncture of the fuel-tank wall, whereas the ignition of fuel by hot spots on tank walls due to lightning strikes is unlikely. Punctures of fuel-tank walls by artificial-lightning discharges produced explosions of the fuel in the mixture range from excessively lean to rich mixtures. None of the aluminum alloys, 0.081 inch thick or over, were punctured by the laboratory discharges representative of natural-lightning discharges to aircraft; however, reliance on this wall thickness for complete protection would not be justified, because occasional strokes are known to be of greater magnitude and because statistics reveal variations in the damage pattern.

Data gathered by the Lightning and Transients Research Institute on lightning strokes to aircraft show that 90 percent of the strokes recorded have occurred in the temperature range of -10° to $+10^{\circ}$ C, where many of the jet fuels are flammable but where aviation gasoline is overrich. Also, 10 percent of the strokes recorded have been to the wings, which are the principal fuel-storage areas for modern aircraft. Thus, there is a hazard, particularly for jet fuels. Certain protective measures are indicated by the studies to date, such as the use of lightning diverter rods, thickening of the wing skin in areas near the most probable stroke paths, and the use of fuel-tank liners in critical areas.

INTRODUCTION

Aircraft flying in thunderstorm regions occasionally are struck by lightning, and the striking of a fuel tank may result in a fire or

explosion. A research program has been undertaken to evaluate this hazard by studying the basic mechanisms of fuel-tank ignition from lightning strokes in various environmental and flight conditions. The phases for which there is limited operating experience are especially emphasized; for example, the operational hazards arising from the use of jet fuels and of wingtip fuel tanks.

The characteristics of natural-lightning discharges to aircraft have been studied by the Lightning and Transients Research Institute (LTRI) through flight research programs, lightning-damage questionnaires, and the analysis of many damaged aircraft parts submitted for inspection by airlines and by the military services over a period of years. The data obtained indicate that a substantial number of strokes to aircraft involve electrical charge transfers as large as 200 coulombs but have relatively low current magnitudes and rates of rise of current. This suggests, as might have been expected, that many strokes to aircraft are of a cloud-to-cloud nature, but it does not preclude the possibility that a stroke to ground may be intercepted by an aircraft. Modern airliners usually fly over or through the upper regions of thunderstorms rather than under them where strokes to ground occur, except, of course, during the landing or takeoff periods.

Owing to the long path lengths of natural-lightning discharges, which may extend for many miles, the resistance of any short length of the path has little effect on the magnitude of the current, so that the discharge can be considered to originate from a constant-current generator. Therefore, the energy developed in an object depends mainly on the resistance (since the energy release is equal to $\int I^2Rt$, where I is the current, R the resistance, and t the time of discharge). Thus, considerably greater energies are released in resistive materials than in metals. For example, strokes to radomes produce damage over areas several feet in diameter, whereas strokes to metal aircraft skin seldom produce holes larger than an inch in diameter.

Aircraft parts that have been damaged by lightning show two general types of pitting. Strokes occurring toward the front parts of aircraft sections are swept to the rear by the motion of the plane; and, as the aircraft passes the relatively stationary ionized channel, small pit marks or holes are burned along the surface or edge. The energy is released over a relatively large area, so that it produces only a small amount of pitting at any one location. Strokes occurring directly to the front, and particularly those to the rear, of a section tend to hang on at a single point for a large fraction of the stroke duration and thus produce larger holes and more severe pitting.

When the lightning strokes are swept to the rear by the relative motion of the aircraft with respect to the stroke channel, the metal aircraft skin is frequently not punctured and the question naturally arises

whether a stroke that does not puncture a fuel-tank wall will cause ignition by heating of the wall. This was considered to be an important question concerning the degree of hazard, and a theoretical and experimental study of fuel-tank wall temperatures due to lightning currents was undertaken at the beginning of the investigation.

Other factors to be considered include the evaluation of the types and magnitudes of discharges required to puncture various fuel-tank walls, the conditions under which a subsequent explosion or fire can occur, and the effects of environmental conditions, fuel types, and fuel-tank location on explosion probability.

This investigation was carried out at the Lightning and Transients Research Institute under the sponsorship and with the financial assistance of the National Advisory Committee for Aeronautics.

APPARATUS AND PROCEDURE

The Lightning and Transients Research Institute (LTRI) has developed artificial-lightning-generation facilities that are particularly suitable for reproducing lightning effects on aircraft as determined by flight research programs made in cooperation with civilian airlines and the military forces. The photograph and cross section of the laboratory (fig. 1) show the location of the high-voltage facilities and the large door for bringing voltage outside the building to test objects such as the aircraft in the foreground.

LTRI facilities for lightning studies include a 5-million-volt impulse generator capable of producing a standard AIEE 1.5×40-microsecond voltage wave (1.5 microsec to crest, 40 microsec to half voltage) and a high-current generator producing a 10×20-microsecond standard AIEE current wave of over 100,000 amperes peak. Mixing the high-voltage and high-current generators makes it possible to reproduce some of the effects found in the lightning-damaged aircraft components studied. However, a comparison of these effects and the data from the flight research program shows that most lightning strokes to aircraft involve much larger charge transfers than are produced by the high-voltage and high-current waves heretofore adopted as lightning test standards in the power industry.

For producing the high charge components of the natural-lightning strokes, two additional generator facilities are used. One of these units consists of a 3000-microfarad bank of 10-kilovolt capacitors which, with appropriate wave-shaping inductance and resistance, produces a 2,000-ampere current of 20-coulomb charge transfer. The second unit consists of a source of 200 amperes d.c. that can be drawn at a source voltage of either 400 or 13,000 volts, depending on the length of the arc it is required to sustain. This unit reproduces the low-current, long-duration components of lightning discharges that have currents of the order of a few hundred amperes.

A schematic circuit diagram of all the generators with their composite lightning-discharge current waveform is shown in figure 2; and the effects of the various stroke components of the three current generators, which are the most important for metal fuel-tank damage studies, are tabulated in table I. The heating effects are given in terms of a multiplying factor for a given resistance. It is interesting to note that both the high-current and the long-duration low-current generators produce much less heating effect than the generator with intermediate current and charge transfer. The three units together produce the major characteristics of lightning strokes: large mechanical forces from the high initial current, a large amount of short-duration heating and blast effects from the intermediate currents, and erosion and pitting effects from the large coulomb transfers of the long-duration low current. The high-voltage generator can be used in conjunction with the current generators, but since it does not contribute significantly to the damage, it is more often used separately to determine the most likely points on aircraft sections or models that the lightning discharges will strike.

For model fuel-tank explosion studies a cylindrical steel tank, 9 feet in diameter and 15 feet high, was constructed to contain explosions and to permit evacuation for altitude testing. A blower supplied by the NACA was connected to the tank for studying windstream effects, and a wind-tunnel section was constructed through the tank interior as illustrated in figures 3 and 4. A 6- by 6-inch cross section at the tunnel throat produced the desired wind velocity of 300 mph. The tank was constructed with large, thick windows for photographic use and special high-voltage bushings for introducing high-voltage discharge at reduced air pressures corresponding to high altitudes. A short plenum chamber, packed with 2-inch furnace pipe to straighten out the airflow, was constructed to join the exponential section that reduced to the Plexiglas throat. A Pitot-static tube and airspeed indicator were used to calibrate the tunnel; a constant velocity of about 300 mph was indicated over most of the throat area. One section of the throat was left open to receive the fuel tanks.

Measurement equipment included an NACA recording mixture analyzer, a potentiometer for thermocouple temperature measurement, an oscilloscope for measuring fuel-tank pressures as determined with a piezoelectric gage, and other miscellaneous equipment, all located outside the tank for protection from the explosions. Much of this equipment was electrically grounded to the tank; and, since the impulse ground-conduction currents raised the tank itself to substantial voltage, an isolation transformer was used to feed all equipment requiring a 115-volt source. A carbon dioxide fire extinguisher was attached to the outside of the tank with a nozzle connected through the wall, aimed at the fuel-tank sample. Thus, any fires following fuel-tank explosions were easily extinguished from the camera operator's position. The scale fuel-tank explosion tests gave

as much difficulty as any high-voltage experiments made in this laboratory because of the large amount of equipment involved and the many test-run failures before the first successful tests were made.

The operations included energizing the 13.8-kilovolt substation to obtain sufficient power for the wind-tunnel blower, charging the three artificial-lightning generators used to produce the composite discharge, setting the automatic timing devices for limiting the long-duration low current, resetting the many overload circuit breakers, measuring fuel-air ratio and temperature, and adjusting cameras and miscellaneous equipment such as lights, and so forth. Although successful test runs required careful setups for each test and good coordination from the operators, it was felt that further construction to obtain completely automatic operation was not justified for the number of tests contemplated.

Gasoline explosions of fuel tanks, even partially filled, constitute a severe fire hazard; and, since explosions of full-size tanks were felt to be a necessary part of the studies, provisions were made for reducing the hazard to a minimum by confining possible explosions. A large pit with concrete-block walls was constructed to confine the explosions to a space next to the building beside the door where voltages and currents could be brought out with relatively short leads, as illustrated in figure 5. The 40-foot-square door allowed maximum voltages to be brought out to the pit test area. The 150-horsepower blower installed in the pit behind suitable asbestos or block barricades provided the necessary flow of air over the tank surface.

A special foam fire-extinguisher system for protecting the area was installed, consisting of a 1,000-gallon tank located at the top of the laboratory building; a centrifugal pump, adding 100 pounds pressure to the 20-pound tank head; foam supply and foam proportioner; two large foam nozzles at each end of the pit, having capacities of 110 gallons per minute each; and the required 2- to 3-inch connecting pipes. For extinguishing localized fires and protecting the laboratory building, a 100-foot auxiliary hose that can be equipped with either a foam playpipe or a water-fog nozzle was provided. The capacity was sufficient to cover the floor of the pit with about 0.7 foot of foam. This system was considered adequate to extinguish possible fires, but the local community fire department could also be called immediately for additional protection in the event that the limited water supply proved to be inadequate.

The control and observation area in the building is indicated in figure 5. All high-voltage controls as well as fire-extinguishing controls and voltage and current waveshape monitoring equipment are located in this area. Two cameras were used in recording the tank explosions, a 16-millimeter motion-picture camera located near the pit and a Fastax camera located on the building roof. The Fastax camera recorded any phenomena that occurred too rapidly for accurate recording by the standard movie camera.

RESULTS AND DISCUSSION

Measurement of Fuel-Tank Wall Temperature

A lightning stroke hitting the outer surface of a fuel-tank wall or of a structural member containing fuel vapors may puncture the wall with a good probability of producing explosion and fire; if the wall thickness is too large to puncture, the stroke increases the temperature of the inner surface of the wall. The stroke will usually cause a small crater of molten metal to form in the outside of the wall, which produces pitting of the surface. Part of the molten metal is displaced by the explosive force of the sudden heating, but part solidifies to add to the heat flowing into the wall. The temperature of the inner surface attains its maximum value directly under the point of stroke contact and decreases rapidly at other points along a radial line from this point on the inner surface. The purpose of this section is to determine, both theoretically and experimentally, possible temperature-time curves for points on the inner surface of a fuel-tank wall when lightning strikes the outer surface. The hazard due to these "hot spots" is evaluated in a later section. Symbols used are defined in appendix A.

When a discharge hits a plate and does not puncture it, the heat is conducted to the inner surface, raising the temperature of that surface, and is also conducted radially from the point of stroke contact and dissipated in the remainder of the plate. In the theoretical study of the heat flow in a plate (appendix B), a block on the surface of the plate of depth β and of square cross section is assumed to be instantaneously heated to a uniform temperature which, for a lightning discharge, is taken to be about 1,200° F, the melting temperature of aluminum. The heat flow from the block into the plate is then calculated from the heat-conduction equation to obtain the temperature at any point in the plate as a function of the time. The calculations are simplified by computing only the temperatures on the inner surface and by letting the breadth of the plate approach infinity, since the size of the plate does not materially affect the heat flow to the inner surface so long as the thickness is small compared with the other dimensions of the plate. Graphical examples giving the numerical results obtained by using these solutions for a hot spot directly under the discharge and for a point near this spot are also presented in appendix B.

Temperatures were measured experimentally in the large cylindrical environmental chamber shown in figure 6 so that the effects of temperature, airstream, and altitude could also be studied. The simulated discharge was directed to the test plate through the high-voltage bushing in the top of the tank. A block diagram of the thermocouple system is shown in figure 7. The thermocouple wires had to be carefully shielded in the vicinity of the tank. Two shields, insulated from each other and

connected only at one point, were used between the thermocouple box and the wall of the chamber. The outer shield carried the heavy discharge currents to the wall, while the inner shield provided additional shielding from electric fields and from any possible unsymmetrical current distribution in the outer shield. The thermocouple voltages were transmitted to the amplifiers and recording equipment in a multiconductor shielded cable.

The instrumentation for these measurements was set up to measure peak temperatures from about 500° F, roughly the spontaneous-ignition temperature of JP-4 fuel, to about 1,200° F, the melting point of aluminum. The oscillograph was considered the best method of recording the rise and decay of the temperature-time curves and the peak temperatures. Iron-constantan thermocouples with size 36 wire were selected for this purpose because of their adequate sensitivity, availability, and sufficiently low thermal inertia to permit accurate measurement of temperature variations at a point. A box about 7 inches square and 2 inches deep shielded the thermocouples from the large simulated-lightning discharge current. Test plates of various representative wall thicknesses were used as top covers for the box, and simulated discharges were directed to the center of the plate. The thermocouples were placed at a point directly beneath the center of the plate and on a radial line from this point. The thermocouple voltages were amplified by d-c amplifiers having a 9-megohm input impedance. The amplifier outputs drove Brush recorders with an over-all sensitivity of about 33° F per millimeter of pen deflection. The maximum chart speed of the recorder was 71 inches per minute, or about 34 milliseconds per millimeter of chart movement. A selector switch was provided for viewing or recording waveforms on a single-channel cathode-ray oscillograph.

The theoretical results of appendix B indicate relatively low temperature peaks at points other than the point directly under the discharge, and the explosion test results of the following section indicate that wall punctures caused explosions but that there were no explosions definitely attributed to inner-wall heating. For this reason most measurements were taken at the point directly under the discharge. The theoretical temperature-time curve for the inner surface of a 1/8-inch aluminum plate with a block, uniformly and instantaneously heated to the melting point of aluminum, was calculated from the equations and curves developed in appendix B. The block was assumed to be in the outside surface of the plate, 0.5 centimeter square and 0.159 centimeter (1/16 in.) deep.

Fifteen high-current discharges were used in the experimental phase of the wall-temperature study. A cross section through the center of an actual crater obtained by discharging a laboratory lightning stroke to a 1/8-inch aluminum test plate is shown in figure 8. This crater is about

0.045 inch deep because of molten metals that have been spattered from the point of stroke contact. However, some of the metal below the crater floor was also heated to the melting point, perhaps to a depth of about 1/16 inch or one-half the wall thickness.

The theoretical temperature-time curve for a 1/8-inch aluminum plate is shown in figure 9(a), and the corresponding experimental curve is shown in figure 9(b). The two curves agree reasonably well. The rise times of the two curves are about the same. The slightly delayed, higher and longer peak of the experimental curve was probably due to the latent heat of fusion of the molten aluminum not displaced, which would tend to store heat at a constant temperature, and also to the fact that the discharge was not applied instantaneously but supplied heat to the plate continuously for about 20 milliseconds. The slightly higher tail on the experimental curve at the longer times can be accounted for by the relatively large ratio of the source size to the size of the thermocouple box used in the experimental setup, since an infinite plate size was assumed for the theoretical calculations. An important experimental parameter that could be investigated is the effect of an airstream on the heat flow to the inner surface. This factor should considerably reduce the hot-spot temperatures measured.

In the curves shown in figure 9 the reference temperature θ may be taken as the temperature of the molten aluminum; thus, in the experimental case, the hot-spot temperature rises to about 530° F in about 30 milliseconds and decays to one-half value in 0.4 second from $t = 0$. As the tank wall thickness decreases, the inner-surface peak temperatures will increase until the thickness at which puncture occurs is reached. While the results of the sample fuel-tank tests show that puncture is the most important factor in causing fuel ignition, it would be of interest to determine the transient temperature-time impulse curves required for ignition of common fuels used in aircraft, as discussed in the following section.

Fuel-Tank Explosion Studies

To determine the specific conditions under which fuels can be ignited, 6-inch-cubic aluminum tanks partly filled with aviation gasoline or JP-4 were struck with 75 high-current discharges over a temperature range from 32° to 90° F. In formulating the problem, consideration was given by NACA and LTRI to the following possible mechanisms for igniting fuels:

(1) The fuel is ignited by a hot spot on the wall of an unpunctured tank.

(2) The discharge penetrates the tank and appears on the inside to produce the equivalent of spark ignition.

(3) An efflux of fuel-air mixture out of the puncture exposes the fuel to the lightning outside the tank. The fire then propagates through the puncture to the inside of the tank.

(4) Incandescent metal particles shower into the tank when the lightning strikes the wall.

Many lightning strokes to aircraft are swept over the surface of the aircraft, and frequently pitting occurs without actual puncture of the skin. It is of considerable interest, therefore, to determine whether hot spots on a fuel-tank wall due to lightning that does not puncture the wall could cause ignition. The temperature-time parameters pertinent to mechanism (1) were considered in the preceding section. The temperature-time graphs for an aluminum tank wall 1/8 inch thick (fig. 9(b)) indicate that for the experimental 20-coulomb discharge the inner-wall temperature will exceed 480° F for only about 60 milliseconds. This is approximately the slow spontaneous-ignition temperature of kerosene or JP-4 and corresponds to about four-tenths of the outer aluminum wall melting temperature of 1,216° F. The investigations of reference 1 show that ignition of methane-air and hydrogen-air mixtures in 40 milliseconds by hot wires requires temperatures estimated to exceed 2,400° F and possibly as high as 3,500° F, an increase of 5 times the slow spontaneous-ignition temperatures.

The experimental discharges were 20 milliseconds in duration. Strokes to the side wall of an exposed aircraft fuel tank should not hang on to any one point on a smooth surface for longer than 10 milliseconds because of the aircraft motion. Pit marks from strokes to aircraft that have been swept over a wing or fuselage surface are generally spaced from a few inches to a few feet apart. Assuming an aircraft velocity of 140 mph or 205 feet per second, this would correspond to a maximum time duration at any single point of 2 feet/205 feet per second = 9.8 milliseconds. Thus in view of the short stroke durations, windstream cooling effects, and resultant lower expected fuel-tank wall temperatures, it seems improbable that strokes that do not puncture should ignite aircraft fuels. It should be emphasized, of course, that this applies only to strokes that are swept and not, for example, to strokes that hang on to the trailing edge of a section and may easily last for periods approaching 1 second. Additional data on the short-time ignition temperature characteristics of aircraft fuels are required for greater assurance on this point.

From the preceding considerations the question naturally arises whether, for short-duration stroke energies slightly below the level required to puncture the tank wall, the metal will be nearly molten and the temperature be high enough to ignite the fuel. It is conceivable that, while the temperatures would greatly exceed the slow spontaneous-combustion temperature of the fuel, the time duration would be too short for ignition. In order to investigate this possibility, a series of tests was made on the 6-inch-cubic tanks of 0.040- and 0.064-inch thickness using stroke energies at approximately the puncture energy level, in which 53 discharges were fired to the series of tanks. The strokes punctured the tanks 16 times and failed to puncture them 37 times. In every case a puncture was accompanied by an explosion, and in every case but one a failure to puncture produced no explosion. The results of these tests were verified in succeeding tests on other phases of the problem. The one explosion that occurred without fuel-tank puncture was due to a discharge that accidentally struck the tank a few inches from a vent hole and possibly threw a spark into or near the opening.

A photographic sequence of fuel-tank ignition by an artificial-lightning discharge that punctured the tank wall is shown in figure 10, as recorded by a Fastax camera. The discharge contacted the rear of the tank, burned a hole through it, and ignited the mixture within a few milliseconds. A similar sequence is shown in figure 11 for a 300-mph windstream and with the electrode on top of the tank. Although a longer time was required for puncture of the second tank, the explosion flamefront velocity appears to be about the same for each case, as does the time required for the tanks to explode, which is less than 40 milliseconds. The mixtures in each tank were fairly close to optimum.

A sketch of the test arrangement for these fuel-tank studies is shown in figure 12. The fuel-air ratios were held in the explosive range during the tests as recorded by the NACA fuel-air analyzer. Temperatures of the fuel were controlled and recorded. The fuel-air ratios were controlled by bleeding air slowly into the tank until the proper mixture was obtained. Owing to the 40-second delay of the mixture analyzer in recording the fuel-air mixture, the mixture rates of change were kept low to minimize interpolation errors. The tanks were normally filled not more than 1/4 inch with fuel. Examination of the areas where the discharges occurred without puncture invariably disclosed fine cracks, probably due to the local heating and cooling, that extended through the tanks and permitted fuel to leak out. These are not considered to be serious, since they probably occurred after the metal had cooled and no external fires occurred. A photomicrograph of one of these areas is shown in figure 13.

Next, a series of tanks was punctured by heavy discharges while the mixture was varied. In nearly every case the tank exploded over a range

of mixtures from 0 to 100 and 100 to 160 extrapolated beyond the normal analyzer range of 0 to 100 parts per thousand. The analyzer was examined to determine whether the indications were incorrect, but pure air produced a reading of zero and warm fuel in the tank drove the analyzer off scale past 100. In addition, explosion pressures were measured for a range of mixtures. The pressures were higher inside the 60 to 80 range, generally bursting the tanks and roughly confirming the accuracy of the mixture analyzer. Only JP-4 was used in investigating hot-spot ignition of fuels, since it was conveniently in the explosive range at room temperature and also had a low spontaneous-ignition temperature; but both JP-4 and 100/130-grade aviation gasoline were used in the pressure measurements. Explosion of the tanks at extremely lean mixtures was attributed to nonequilibrium conditions: a lean mixture in the space over the fuel which the analyzer sampled, and a combustible mixture at the fuel-air boundary ignited by spark showers from the puncture. Photographs of spark showers from punctured aluminum sheets are shown in figure 14.

To measure overrich mixtures, which were not measured by the mixture analyzer, specific mixtures were obtained by allowing partially filled fuel tanks to come to equilibrium at particular temperatures. For example, tanks with gasoline held for 5 minutes at 80° F were assumed to contain an extremely overrich mixture. Puncturing discharges did not cause an explosion, but a fire was started at the puncture hole that continued for 1 minute until put out by an extinguisher. Gasoline held at 32° F did not explode; however, JP-4 did explode at this temperature. Discharges below the liquid level produced fires at the puncture point but no explosions.

In analyzing the sequence of explosion experiments, the mechanisms listed at the beginning of this section that appear the most likely are the direct puncture of fuel-tank walls followed by (2) explosion and (3) external fires. Ignition by (1) hot spots seems improbable on the basis of the investigations of the preceding section, and (4) the showering of sparks into a tank with no puncture would be even more improbable, since the wall would probably not be hot enough to spark if it would not ignite the fuel.

Although initial measurements indicated that lightning-discharge currents because of their great energies were capable of igniting fuels over a greater range of mixtures than would be possible with spark ignition, particularly with lean mixtures, basically the investigations showed general agreement with existing flammability data. Overrich mixtures were not exploded, but external fires occurred at the puncture holes. Lean mixtures were ignited, but ignition of lean mixtures due to mists (e.g., from agitation) has been generally recognized. The explosion hazard is considered to be more serious than the fire hazard. External fires can occur whenever a fuel-tank wall is punctured, with any

fuel; but aircraft fires, though a serious matter, can often be controlled. Because of the low flame-propagation rates under any but extreme conditions, these fires are sometimes extinguished by the windstream, sometimes by special maneuvers of the aircraft, or by carbon dioxide systems. Explosions of fuel tanks, on the other hand, can result in severe structural damage or loss of the aircraft. For this reason, the most significant information regarding the degree of hazard is probably the relation of the flammability ranges of various fuels to the temperatures at which most lightning strokes to aircraft occur.

LTRI records show that, for 109 lightning strokes to aircraft on domestic flights, 93 percent occurred within 10° C of the freezing temperature, or from 14° F to 50° F. This temperature range includes the flammability range of JP-4, is below the lean limit for JP-5, JP-1, or kerosene, and includes the rich region for JP-3 and the extreme overrich range for aviation gasoline. Thus, the safest fuel with respect to lightning hazards would be aviation gasoline, with JP-4 the worst. The safety of JP-1 and JP-5 appears to depend on how readily they form mists; also, the precise mechanism by which LTRI obtained explosions of lean mixtures needs further clarification.

The experimental results have been confirmed by recent flight-damage reports of lightning strokes to aircraft fuel tanks. Holes in tanks from lightning, a gasoline fire in one tank that burned for 15 minutes, as well as an explosion of a jet aircraft wingtip fuel tank just after it had been jettisoned have all been reported within the last nine months. Thus, no other conclusion can be reached but that jet fuels, JP-4 in particular, present a much more severe explosion hazard than aviation gasoline, which has shown a good safety record to date.

Metal Erosion from Lightning Discharges

In order to determine the energies and charge transfers required to puncture various thicknesses of aircraft aluminum alloys, 75 high-current laboratory discharges with and without windstream were fired to test samples of three alloys commonly used for fuel-tank walls. The alloys were 2024-T3, 3003-H14, and 6061-TS in 0.020-, 0.040-, 0.064-, 0.081- and 0.102-inch thicknesses. A tapered double-wall construction was used with the two thinnest samples to examine the relative merits of double-wall construction against single walls of equivalent thickness. The walls were spaced 1/8, 1/4, 1/2, and 1 or more inches apart. The artificial-lightning discharges discussed in the APPARATUS AND PROCEDURE section were used together to produce a single standard combined discharge. As discussed previously, the predominant factor in puncture of aluminum tank walls is the charge transfer of the long-duration low currents and of the intermediate currents; however, since the metal erosion for a given

charge transfer is modified to some extent by the current magnitude, relating metal erosion to charge transfer is of course an approximation. Holes burned in the ends of wingtip tank tailcones by natural lightning (fig. 15(a)) can be compared with holes produced in aluminum sheet by laboratory discharges (fig. 15(b)). In the 30-coulomb laboratory discharges, the hole size varies considerably with the current magnitude. The standard discharge that LTRI has adopted as representative of strokes to aircraft will duplicate most of the damage done to aircraft, but it should be noted that occasionally there will be strokes that may exceed 200 coulombs by a considerable amount.

The combined artificial-lightning discharges fired to the various alloys produced punctures in all thicknesses through 0.064 inch but in none of the alloys 0.081 inch or over with the exception of some in the windstream tests in which the vibration caused the arcing electrode actually to contact the aluminum sheet. Owing to difficulty in maintaining the arc with the airflow present, the windstream tests were not considered to be representative of natural-lightning discharges under windstream conditions, since the arc was confined to one point, but they did provide valuable information regarding cooling and other secondary effects. Use of higher potential long-duration current sources and a larger wind-tunnel section would permit longer arcs that would be more representative of natural-lightning discharges to aircraft; however, this would not produce conclusive information as to hazard, because the variation in natural-lightning discharges is so great that no reasonable value of stroke magnitude can be selected as a "probable expected maximum." Discoloration and heat distortion of the metal, noted when no windstream was used, were almost totally absent with the windstream, indicating an extensive cooling effect; the metal erosion was clean and slightly more severe, apparently because of the plentiful supply of oxygen. It is interesting to note that flight-damage reports have mentioned similar effects; for example, one reported that "burned spots on the tank resembling momentary touches by a cutting torch clearly indicate that damage was done by a lightning strike." In tests of double-wall sections, 0.040-inch aluminum had to be separated 1/4 inch to be equivalent to one 0.081-inch wall, and double-wall sections of 0.020-inch aluminum were punctured when separated over $1\frac{1}{2}$ inches. Photographs of the effect of the discharges on aluminum sheet are shown in figure 16.

The knowledge of the sweeping effect of the aircraft motion in reducing the localized pitting by distributing the stroke energy over a large area had earlier permitted some optimism regarding the need for lightning protection of fuel-tank side walls. As an example, the effect of aircraft motion in sweeping natural-lightning discharges is illustrated in figures 17 and 18. In the tip tank tailcone shown in figure 17, two small pit marks are shown on the side wall, but a moderate-sized hole may be seen at the rear where the stroke could hang on for an extended period.

Holes in 0.020-inch aircraft skin are shown in figure 18. The stroke apparently struck a long wire antenna attached to a VHF mast located at the left and was conducted along the wire and down the mast to the base where it burned a large hole as the aircraft moved forward. At this point it probably broke away from the mast to burn the series of small holes in the thin aluminum sheet.

Although the standard laboratory discharges considered to be representative for aircraft struck in flight did not puncture aluminum sheet 0.081 inch thick, it is felt that complete reliance on this wall thickness for protection from natural strokes to aircraft would not be justified because of the occasional strokes that are known to contain considerably greater charge transfers than the 200 coulombs used in this sequence of tests. Although the probability of such a discharge to a fuel-tank side wall is small, the consequences are so serious that additional precautions are felt to be necessary. Such additional precautions could include ribs on tip tanks, location of tanks away from the immediate tip area where lightning strokes are most likely to occur, use of fuel-tank liners in critical areas near the wingtip, or thickening of the wing and use of lightning diverters to divert strokes from critical areas such as fuel vents.

Lightning Strike Data Pertinent to Fuel-Tank Hazards

In the preceding sections of this report, references have been made to LTRI data on lightning strokes to aircraft. Pertinent sections of these data are presented in figures 19 to 21. The distribution of lightning strokes with temperature for domestic airline flights is shown in figure 19. Over 90 percent of the strokes for which the temperatures have been recorded occurred within the range of $+10^{\circ}$ to -10° C, and 65 percent of the strokes occurred in the range of 0° to $+5^{\circ}$ C. This is not surprising in view of the most widely accepted theory of thunderstorm electrical charge formation by separation across the freezing level.

It has been suggested that the strokes are grouped about the freezing level because it happens to correspond to the most common flight altitudes. The LTRI data on the distribution of strokes with altitude (fig. 20) disproves this theory. These data, which show that the strokes occurred at no particular altitudes, indicate that the probability that an aircraft will be struck is related to its proximity to the freezing level. Most strokes occurred at altitudes of 6,000 feet or over where the cloud-to-cloud discharges of low-current magnitudes and high-charge transfers are more common. This is in agreement with the analysis of lightning-damaged aircraft parts, which shows that a substantial proportion of such parts have passed high-charge transfers.

The analysis of the distribution of damage presented in figure 21 shows that a substantial percentage of strokes occurred to the wings, which in modern aircraft are the principal fuel-storage locations. Figure 21 is based on 431 incidents, which is considerably more than for figures 19 and 20 because most stroke reports received record the part struck but some do not record the temperature or altitude.

Model Studies of Most Likely Points of Lightning Strike

Flight-damage report statistics are a great aid in evaluating hazards because they provide general information as to the most likely points for lightning to strike. Model studies are also effective for studying critical areas of aircraft in some detail. Although extensive model studies were not contemplated in this investigation, preliminary studies in another investigation indicate that, for the wings, the most vulnerable areas are the tip areas and the areas behind the propellers on propeller-driven aircraft. Direct strokes to the wingtip and strokes to the propellers that can be swept back by the airstream over either the top or bottom of the wing are most probable. Two-million-volt discharges to model aircraft are shown in figures 22 to 24. Discharges to two model aircraft (figs. 22 and 23) illustrate the high probability of vertical strokes to the vertical fin. Strokes to the model from various angles permit evaluation of the most probable points of lightning strike; and, by use of intermediate-sized model sections, somewhat more detailed information may be obtained. This information, as related to the airflow direction, permits fair estimates of protection in these critical areas.

The streamer on the wingtip of the aircraft in figure 23 illustrates effectively the mechanism of lightning-stroke approach to an aircraft. When the advancing step leader of a lightning stroke nears the aircraft, an intense electric field is set up and corona streamers produced by this field leave the aircraft from high-gradient points to meet the step leader. The step leader contacts the aircraft through one or more of the streamers and raises the aircraft potential to a value sufficient to produce streamers off the opposite aircraft extremities. These streamers form the step leaders for further advance of the stroke past the aircraft. The formation of streamers is determined by the extent of the field distortion about the aircraft. Their formation near the aircraft is probably affected by the pressure variations caused by local turbulence; however, this has not been definitely established.

Electrolytic tank plots of the electric-field configuration about the aircraft model also give a clear picture of the extent of the field distortion, which is only indirectly illustrated by photographs of strokes to a model. An electrolytic tank plot of the electric field about the model of figure 24 is shown in figure 25 just before and after a lightning stroke contacts the aircraft. The extent and intensity of the

electric field are maximum about the nose and wingtip fuel tanks, as indicated by the spacing and shape of the equipotential lines. This is in agreement with the high-voltage studies, which showed about equal probability for strokes to the aircraft nose or front of the wingtip tank (fig. 24). More extensive studies of this type would be valuable in general development of protective measures, especially in studies of particular areas of specific aircraft.

CONCLUDING REMARKS

This experimental investigation of the various mechanisms of fuel-tank explosion due to lightning strokes reveals that there is a primary hazard whenever there is direct puncture of the fuel-tank wall but that the ignition of fuel by hot spots on tank walls without puncture is unlikely. Punctures of the fuel-tank walls by artificial-lightning discharges under various environmental conditions produced explosions of fuel mixtures varying from excessively lean to full-rich. When a hole was not actually made in the inner fuel-tank wall, temperatures exceeded one-half the exterior molten-aluminum temperatures only for brief periods, probably insufficient to cause explosion of aircraft fuels. Additional data on the short-time ignition temperature characteristics of aircraft fuels are required for complete assurance on this point.

LTRI data on lightning strikes to aircraft show that 90 percent of the strikes recorded have been in the temperature range from -10° to $+10^{\circ}$ C, where many of the jet fuels are explosive but where aviation gasoline is overrich. Also, 10 percent of the strokes recorded have been to the wing areas, which for modern aircraft are the principal fuel-storage areas. These results indicate that protective measures are needed, particularly for jet fuels and to a lesser extent for aviation gasoline, which, although not explosive in the temperature ranges at which most lightning strokes occur, can be ignited to produce external fires.

Fuel-tank aluminum alloys 0.081 inch or thicker were not punctured by discharges representative of natural-lightning discharges to aircraft. However, reliance for protection from aircraft lightning strokes solely on increasing tank thicknesses to 0.081 inch is not necessarily a solution, since occasional strokes are known to contain considerably greater charge transfers than the 200 coulombs used in the experimental studies. Although the probability of such strokes to critical areas is small, the consequences - possible fires or explosions - are so serious that additional precautions are felt to be necessary.

While protection-system development is beyond the scope of this report, the following suggestions can be made for development of protective measures:

(1) Some thickening of specific tank areas or use of external fins or ribs to be located on the basis of the probability of discharge paths may considerably reduce the hazard.

(2) Several types of fuel-tank liners may be used adjacent to the most probable discharge path.

(3) Lightning-diverter rods may be used to divert strokes from critical areas such as fuel vents.

(4) Blowout panels may be used in tanks near the wingtip to reduce the stress on the main wing structure due to a tank explosion near the tip.

(5) Plastic wingtip tanks, though considered quite hazardous without specific protective design, might be made safer than conventional metal tanks.

Lightning and Transients Research Institute,
Minneapolis, Minn., February 1, 1957.

APPENDIX A

SYMBOLS

A	coefficient in Fourier series
a	length of side of plate
b	thickness of plate
C	capacity
c	specific heat
E	voltage
I	current
k	thermal conductivity
l,m,n,p	non-negative integers
Q	quantity of heat
R	resistance
T	temperature
t	time
t'	time constant $t' = b/\pi\varkappa^2$
u	temperature at $t = 0$
x,y,z	rectangular coordinates
α	length of side of heated block
β	depth of heated block
$\delta_{l,0}$	Kronecker symbol (defined in eq. (14))
θ	reference temperature rise (initial temperature of heated block)
$\varkappa^2$	thermal diffusivity

ρ density

∇^2 differential operator $\left(\nabla^2 = \frac{\partial^2}{\partial x^2} + \frac{\partial^2}{\partial y^2} + \frac{\partial^2}{\partial z^2}\right)$

APPENDIX B

HEAT FLOW IN A PLATE DUE TO LIGHTNING STROKE

Introduction

When a lightning stroke hits a metal plate, such as a structural member of an airplane, it may burn through the plate or it may burn out only a small pool of metal, causing a pitting of the plate. Of course, the worst damage is caused when a hole is burned through the plate. The material on the back side is then open to damage by the arc; and, if a member such as a gas tank is involved, explosion may result.

Even if the plate is not burned through, there may be a sufficiently great release of heat energy in the plate to lead to severe damage. The question is whether a large enough temperature rise may occur on the inner surface of the wall of a gas tank to initiate an explosion in the tank. This problem in heat conduction is theoretically analyzed herein.

Theory

Consider a metal plate in the form of a square of side a and of thickness b, with $a >> b$. Take a rectangular set of coordinate axes with origin at the center point of one side of the plate, referred to as the inside surface. Orient the x,y-axes parallel to the sides of the plate, and the z-axis normal to the inside surface. The outside surface of the plate then corresponds to the surface $z = b$. The lightning stroke will be supposed to strike the outside surface of the plate at the point $(0,0,b)$, directly opposite the origin of coordinates 0 of the coordinate system, and to release there a quantity of heat Q at time $t = 0$. The problem is to evaluate the temperature distribution on the inner surface of the plate as a function of time; in particular, the temperature at the point 0, which will be the hottest point on the inner surface.

Since this is a damage problem, it is best to set the conditions on the analysis so that the temperature rise on the inner surface will be overestimated rather than underestimated. Therefore, the analysis is simplified by supposing that no heat is lost from the plate either by radiation or by conduction to the air.

The heat-conduction equation

$$\left(\varkappa^2\nabla^2 - \frac{\partial}{\partial t}\right) T = 0 \qquad (1)$$

is to be solved in the region

$$\left.\begin{aligned} \frac{-a}{2} \le x \le \frac{a}{2} \\ \frac{-a}{2} \le y \le \frac{a}{2} \\ 0 \le z \le b \end{aligned}\right\} \qquad (2)$$

with the boundary conditions

$$\left.\begin{aligned} \frac{\partial T}{\partial x} = 0 \quad \text{at} \quad x = \pm\frac{a}{2} \\ \frac{\partial T}{\partial y} = 0 \quad \text{at} \quad y = \pm\frac{a}{2} \\ \frac{\partial T}{\partial z} = 0 \quad \text{at} \quad z = 0,b \end{aligned}\right\} \qquad (3)$$

The following functions are special solutions of the heat-conduction equation (1) that satisfy the boundary conditions (3):

$$\cos\left[\left(\frac{l\pi}{a}\right)\left(x + \frac{a}{2}\right)\right] \cos\left[\left(\frac{m\pi}{a}\right)\left(y + \frac{a}{2}\right)\right] \cos\left[\left(\frac{n\pi}{b}\right)z\right] \exp(-\lambda_{lmn}t) \qquad (4)$$

where l, m, and n are non-negative integers and

$$\lambda_{lmn} = \varkappa^2\left[\left(\frac{l\pi}{a}\right)^2 + \left(\frac{m\pi}{a}\right)^2 + \left(\frac{n\pi}{b}\right)^2\right] \qquad (5)$$

Next, these particular solutions are combined in such a manner that the initial conditions representing the heat source produced on the outside of the plate by the lightning stroke are satisfied. For this purpose the general solution for the temperature at any point in the plate is formed:

$$T(x,y,z,t) = \sum_{l,m,n=0}^{\infty} A_{lmn}\left\{\cos\left[\left(\frac{l\pi}{a}\right)\left(x + \frac{a}{2}\right)\right]\cos\left[\left(\frac{m\pi}{a}\right)\left(y + \frac{a}{2}\right)\right]\cos\left[\left(\frac{n\pi}{b}\right)z\right]\exp(-\lambda_{lmn}t)\right\} \qquad (6)$$

Let the temperature distribution at $t = 0$ be known, so that

$$T(x,y,z,0) = u(x,y,z) \qquad (7)$$

is a known function of the coordinates x,y,z in the plate. Combining equations (6) and (7) gives

$$u(x,y,z) = \sum_{l,m,n=0}^{\infty} A_{lmn} \left\{ \cos\left[\left(\frac{l\pi}{a}\right)\left(x + \frac{a}{2}\right)\right] \cos\left[\left(\frac{m\pi}{a}\right)\left(y + \frac{a}{2}\right)\right] \cos\left[\left(\frac{n\pi}{b}\right)z\right] \right\} \tag{8}$$

In order to express the coefficients in this Fourier series in terms of the function $u(x,y,z)$, the symbol $M[F(x,y,z)]$ is defined as the mean value of the function $F(x,y,z)$ over the volume of the plate. That is,

$$M[F(x,y,z)] = \frac{1}{a^2 b} \int_{-a/2}^{a/2} \int_{-a/2}^{a/2} \int_{0}^{b} F(x,y,z)\, dz\, dy\, dx \tag{9}$$

where $a^2 b$ is the volume of the plate.

Using equation (8) and the usual methods of calculating the coefficients in a Fourier series gives

$$A_{lmn} = \frac{M\left\{ u(x,y,z) \cos\left[\left(\frac{l\pi}{a}\right)\left(x + \frac{a}{2}\right)\right] \cos\left[\left(\frac{m\pi}{a}\right)\left(y + \frac{a}{2}\right)\right] \cos\left[\left(\frac{n\pi}{b}\right)z\right] \right\}}{M\left\{ \cos^2\left[\left(\frac{l\pi}{a}\right)\left(x + \frac{a}{2}\right)\right] \cos^2\left[\left(\frac{m\pi}{a}\right)\left(y + \frac{a}{2}\right)\right] \cos^2\left[\left(\frac{n\pi}{b}\right)z\right] \right\}} \tag{10}$$

The evaluation of the initial temperature distribution $u(x,y,z)$ requires simulating the heating effect of the lightning stroke in some suitable fashion. Suppose that at $t = 0$ an amount of heat Q is liberated in a small block of the plate defined by the conditions

$$\left.\begin{aligned} \frac{-a}{2} < \frac{-\alpha}{2} \le x \le \frac{\alpha}{2} < \frac{a}{2} \\ \frac{-a}{2} < \frac{-\alpha}{2} \le y \le \frac{\alpha}{2} < \frac{a}{2} \\ b - \beta \le z \le b \end{aligned}\right\} \tag{11}$$

The heat is thus liberated in the small block of dimensions α,α,β situated on the outer surface of the plate, just opposite the point 0 on the plate. The material in this block will be raised to the uniform temperature

$$\theta = \frac{Q}{c\rho\alpha^2\beta} \tag{12}$$

where c is the specific heat and ρ is the density of the metal. The function $u(x,y,z)$ will be equal to θ in this block and equal to zero outside it.

The coefficients A_{lmn} from equation (10) can now be evaluated as follows:

$$A_{lmn} = \theta \frac{\left\{\frac{1}{a}\int_{-\alpha/2}^{\alpha/2} \cos\left[\left(\frac{l\pi}{a}\right)\left(x + \frac{a}{2}\right)\right] dx\right\}\left\{\frac{1}{a}\int_{-\alpha/2}^{\alpha/2} \cos\left[\left(\frac{m\pi}{a}\right)\left(y + \frac{a}{2}\right)\right] dy\right\}\left\{\frac{1}{b}\int_{b-\beta}^{b} \cos\left[\left(\frac{n\pi}{b}\right)z\right] dz\right\}}{\left[\frac{1}{2}(1 + \delta_{l,0})\right]\left[\frac{1}{2}(1 + \delta_{m,0})\right]\left[\frac{1}{2}(1 + \delta_{n,0})\right]} \tag{13}$$

For convenience of notation the Kronecker symbols are used:

$$\delta_{l,0} = \begin{cases} 1 & \text{if } l = 0 \\ 0 & \text{if } l \neq 0 \end{cases} \tag{14}$$

Carrying out the integrations indicated in equation (13) yields

$$\frac{1}{a}\int_{-\alpha/2}^{\alpha/2} \cos\left[\left(\frac{l\pi}{a}\right)\left(x + \frac{a}{2}\right)\right] dx = \frac{1}{l\pi}\left\{\sin\left[\left(\frac{l\pi}{a}\right)\left(\frac{a+\alpha}{2}\right)\right] - \sin\left[\left(\frac{l\pi}{a}\right)\left(\frac{a-\alpha}{2}\right)\right]\right\}$$

$$= \left(\frac{2}{l\pi}\right)\sin\left(\frac{\alpha l\pi}{2a}\right)\cos\left(\frac{l\pi}{2}\right)$$

$$= \begin{cases} 0 & \text{if } l \text{ is odd} \\ (-)^{l/2}\,\dfrac{\sin\left(\frac{l\pi\alpha}{2a}\right)}{\frac{l\pi\alpha}{2a}}\,\dfrac{\alpha}{a} & \text{if } l \text{ is even} \end{cases} \tag{15}$$

$$\frac{1}{b}\int_{b-\beta}^{b}\cos\left[\left(\frac{n\pi}{b}\right)z\right]dz = \frac{1}{n\pi}\left\{\sin(n\pi) - \sin\left[n\pi\left(\frac{b-\beta}{b}\right)\right]\right\}$$

$$= \left(\frac{2}{n\pi}\right)\sin\left(\frac{n\pi\beta}{2b}\right)\cos\left[n\pi\left(\frac{2b-\beta}{2b}\right)\right]$$

$$= (-)^{n}\left(\frac{2}{n\pi}\right)\sin\left(\frac{n\pi\beta}{2b}\right)\cos\left(\frac{n\pi\beta}{2b}\right)$$

$$= (-)^{n}\left(\frac{\beta}{b}\right)\frac{\sin\left(\frac{n\pi\beta}{b}\right)}{\frac{n\pi\beta}{b}} \qquad (16)$$

This yields the general formula

$$A_{lmn} = \theta\,\frac{\frac{\alpha^2\beta}{a^2 b}}{\left[\frac{1}{2}(1+\delta_{l,0})\right]\left[\frac{1}{2}(1+\delta_{m,0})\right]\left[\frac{1}{2}(1+\delta_{n,0})\right]}(-)^{[(l+m)/2]+n}\,\frac{\sin\left(\frac{l\pi\alpha}{2a}\right)\sin\left(\frac{m\pi\alpha}{2a}\right)\sin\left(\frac{n\pi\beta}{b}\right)}{\left(\frac{l\pi\alpha}{2a}\right)\left(\frac{m\pi\alpha}{2a}\right)\left(\frac{n\pi\beta}{b}\right)} \qquad (17)$$

Here l and m have only even values, since by equation (15) the coefficient A_{lmn} will vanish if l or m is odd.

The final solution of equation (6) for the temperature distribution in the plate for $t \geq 0$ can be written as

$$T(x,y,z,t) = \frac{Q}{c\rho\alpha^2\beta}\,\varphi(a,\alpha;x,t)\varphi(a,\alpha;y,t)\,\psi(b,\beta;z,t) \qquad (18)$$

where

$$\varphi(a,\alpha;x,t) = \sum_{l=0,2,4,\ldots}^{\infty}\frac{(-)^{l/2}\,\frac{\alpha}{a}\cos\left[\left(\frac{l\pi}{a}\right)\left(x+\frac{a}{2}\right)\right]}{\frac{1}{2}(1+\delta_{l,0})}\,\frac{\sin\left(\frac{l\pi\alpha}{2a}\right)}{\frac{l\pi\alpha}{2a}}\exp\left[-\left(\frac{l\pi x}{a}\right)^2 t\right] \qquad (19)$$

$$\psi(b,\beta;z,t) = \sum_{n=0,1,2,\ldots}^{\infty}\frac{(-)^{n}\,\frac{\beta}{b}\cos\left[\left(\frac{n\pi}{b}\right)z\right]}{\frac{1}{2}(1+\delta_{n,0})}\,\frac{\sin\left(\frac{n\pi\beta}{b}\right)}{\frac{n\pi\beta}{b}}\exp\left[-\left(\frac{n\pi\kappa}{b}\right)^2 t\right] \qquad (20)$$

If l is even,

$$\cos\left[\left(\frac{l\pi}{a}\right)\left(x + \frac{a}{2}\right)\right] = (-)^{l/2} \cos\left(\frac{l\pi x}{a}\right) \tag{21}$$

so that the new summation index, $p = l/2$, can be introduced, which takes all non-negative integral values, and formula (19) can be replaced by

$$\varphi(a,\alpha;x,t) = \sum_{p=0,1,2,\ldots}^{\infty} \frac{\frac{\alpha}{a}\cos\left(\frac{2p\pi x}{a}\right)}{\frac{1}{2}(1 + \delta_{l,0})} \frac{\sin\left(\frac{p\pi\alpha}{a}\right)}{\frac{p\pi\alpha}{a}} \exp\left[-\left(\frac{2p\pi\varkappa}{a}\right)^2 t\right] \tag{22}$$

The formulas given represent the exact solution of the proposed problem. However, in view of the nature of the applications to be made of them, it is feasible to allow some simplifications.

The size of the plate is not very material to the flow of the heat to the inside of the plate so long as the thickness is small compared with the breadth of the plate. It is therefore convenient to take the limit $a \to \infty$. In this case,

$$\varphi(\alpha;x,t) = \lim_{a \to \infty} \varphi(a,\alpha;x,t) \tag{23}$$

The series in equation (22) goes over into an integral, and on working out the process the following solution is found:

$$\varphi(\alpha;x,t) = \frac{2}{\pi}\int_0^{\infty} \frac{\sin\xi}{\xi}\cos\left(\frac{2x\xi}{\alpha}\right)\exp\left[-\left(\frac{2\varkappa\xi}{\alpha}\right)^2 t\right]d\xi \tag{24}$$

where $\xi = p\pi\alpha/a$.

This function can be reduced to a more convenient form for numerical computations. Introduce the following notation (which is valid for $t > 0$):

$$\left.\begin{aligned} \mu &= \left(\frac{2x\sqrt{t}}{\alpha}\right)\xi \\ \xi &= \left(\frac{\alpha}{2x\sqrt{t}}\right)\mu \end{aligned}\right\} \tag{25}$$

Substitution into equation (24) yields

$$\varphi(\alpha;x,t) = \frac{2}{\pi}\int_0^\infty \frac{\sin\left(\frac{\alpha\mu}{2\varkappa\sqrt{t}}\right)}{\mu}\cos\left(\frac{x\mu}{\varkappa\sqrt{t}}\right)\exp\left(-\mu^2\right)d\mu$$

$$= \frac{1}{\pi}\int_0^\infty\left[\sin\left(\frac{x+\frac{\alpha}{2}}{\varkappa\sqrt{t}}\mu\right) - \sin\left(\frac{x-\frac{\alpha}{2}}{\varkappa\sqrt{t}}\mu\right)\right]\frac{\exp\left(-\mu^2\right)}{\mu}d\mu \tag{26}$$

Now define the function

$$g(\eta) = \frac{2}{\pi}\int_0^\infty \frac{\sin(2\eta\mu)}{\mu}\exp\left(-\mu^2\right)d\mu \tag{27}$$

Making use of this abbreviation gives from equation (26),

$$\varphi(\alpha;x,t) = \frac{1}{2}\left[g\left(\frac{x+\frac{\alpha}{2}}{2\varkappa\sqrt{t}}\right) - g\left(\frac{x-\frac{\alpha}{2}}{2\varkappa\sqrt{t}}\right)\right] \tag{28}$$

From equation (27),

$$\frac{dg}{d\eta} = \frac{4}{\pi}\int_0^\infty \cos(2\eta\mu)\exp\left(-\mu^2\right)d\mu$$

$$= \frac{2}{\sqrt{\pi}}\exp\left(-\eta^2\right) \tag{29}$$

on making use of formula 508 of Peirce's table of integrals (ref. 2). It is obvious from equation (27) also that $g(0) = 0$. Equation (29) is integrated directly as a differential equation:

$$g(\eta) = \frac{2}{\sqrt{\pi}}\int_0^\eta \exp\left(-\mu^2\right)d\mu \tag{30}$$

This shows that the function $g(\eta)$ defined in equation (27) is just the ordinary probability integral and thus can be found tabulated in numerical form.

The following formula for the temperature distribution from the heat source (strictly speaking, in a plate of infinite breadth) is finally obtained:

$$T(x,y,z,t) = \frac{Q}{c\rho\alpha^2\beta}\,\varphi(\alpha;x,t)\varphi(\alpha;y,t)\psi(b,\beta;z,t) \tag{31}$$

with the function $\varphi(\alpha;x,t)$ defined by equation (28) and the function $\psi(b,\beta;z,t)$ defined by equation (20).

Discussion of Formula (31)

Formula (31) gives the temperature distribution throughout the plate resulting from the heat source introduced by the lightning stroke. In applying the result, only the temperature distribution over the inner surface needs to be known. This is obtained by setting $z = 0$ in equation (31). For simplicity of notation, this temperature function is written as follows:

$$T_0(x,y;t) = T(x,y,0;t) \tag{32}$$

The following formula results:

$$T_0(x,y;t) = \frac{Q}{c\rho\alpha^2\beta}\,\varphi(\alpha;x,t)\varphi(\alpha;y,t)\psi(b,\beta;0,t) \tag{33}$$

where, from equation (20),

$$\psi(b,\beta;0,t) = \frac{\beta}{b}\sum_{n=0,1,\ldots}^{\infty}\frac{(-)^n \sin\left(\frac{n\pi\beta}{b}\right)}{\frac{1}{2}(1+\delta_{n,0})\left(\frac{n\pi\beta}{b}\right)}\exp\left[-\left(\frac{n\pi x}{b}\right)^2 t\right] \tag{34}$$

Since the temperature distribution $T_0(x,y;t)$ is expressed in equation (33) as the product of two types of functions, it is convenient to examine the nature of each of these functions separately.

At the initial instant $t = 0$, conditions require that the whole of the inner surface of the plate be at the uniform temperature taken to be $T \doteq 0$. Therefore, the following must be obtained from equation (34):

$$\psi(b,\beta;0,0) = \frac{\beta}{b}\sum_{n=0}^{\infty}\frac{(-)^n \sin\left(\frac{n\pi\beta}{b}\right)}{\frac{1}{2}(1+\delta_{n,0})\left(\frac{n\pi\beta}{b}\right)} = 0 \tag{35}$$

This is an alternating series of a type somewhat difficult to handle, since the terms do not diminish very rapidly in magnitude. There will be no attempt to prove rigorously that the sum of the series is actually zero as is indicated in equation (35).

It is apparent by inspection of equation (34) that as $t \to \infty$ the series converges rapidly to the value

$$\psi(b,\beta;0,\infty) = \frac{\beta}{b} \tag{36}$$

Owing to the exponential nature of the summands in the series in their dependence on the time variable, the dominating term will be the one having the smallest exponent; that is, the second member of the series, since the first one ($n = 0$) does not depend on the time at all. Therefore, the function given by equation (34) will start from zero at $t = 0$ and will rise quickly to the final value β/b practically like an exponential function with the time constant

$$t' = \left(\frac{b}{\pi\varkappa}\right)^2 \tag{37}$$

Expressed in physical terms, this function determines the flow of heat from the initial heat source directly through the thickness of the plate. The time constant (37) can therefore be expected to be quite small for plates of ordinary thickness such as are used in the construction of aircraft.

For an aluminum plate,

$$\text{Thermal conductivity} = k = 0.504 \text{ cal/(cm)(sec)}(^\circ\text{C})$$

$$\text{Specific heat} = c = 0.217 \text{ cal/(g)}(^\circ\text{C})$$

$$\text{Density} = \rho = 2.70 \text{ g/cm}^3$$

From this information, the thermal diffusivity is

$$\varkappa^2 = \frac{k}{c\rho} = 0.086 \text{ cm}^2/\text{sec}$$

$$\varkappa = \sqrt{0.86} = 0.93 \text{ cm}/\sqrt{\text{sec}}$$

Taking $b = 1/8$ inch $= 0.318$ centimeter, the time constant is

$$t' = \left(\frac{0.318}{0.93\pi}\right)^2 = 0.0119 \text{ sec} \tag{38}$$

The rise time of the temperature on the inner surface of the plate, directly opposite the heat source, should thus be of the order of 12 milliseconds. This result will not be particularly sensitive to the size of the initial heat source; that is, it does not depend greatly on the value of β, since the expression (37) for t' does not involve this parameter.

The temperature at the point 0 should have a maximum value, which is about

$$T_{0,max} = \frac{Q}{c\rho\alpha^2 b} = \theta \frac{\beta}{b} \tag{39}$$

The initial rise of the temperature at the point 0 is determined by the flow of heat through the thickness of the plate, but its ultimate decline is governed by the transverse flow of heat along the plate. This is expressed by the functions $\varphi(\alpha;x,t)$ and $\varphi(\alpha;y,t)$, which, of course, have the same functional form.

From the initial conditions, the following is expected at $t = 0$:

$$\varphi(\alpha;x,0) = \begin{cases} 0 & \text{if } |x| > \alpha/2 \\ 1 & \text{if } |x| < \alpha/2 \end{cases} \tag{40}$$

It is easy to show from equation (28) that this is the case, if it is noted from equation (30) that

$$\left.\begin{aligned} g(-\eta) &= -g(\eta) \\ g(\infty) &= 1 \end{aligned}\right\} \tag{41}$$

The function $\varphi(\alpha;x,t)$ is roughly exponential in form and decays comparatively slowly in relation to the initial rapid rise of temperature at the point 0. It is best shown in the form of graphs drawn for special cases.

The analysis has assumed that the initial heat source has a square cross section and a depth β. In practice one will have little or no control over the exact shape of the region in which a lightning stroke develops heat in the plate; and on the whole one will probably find a circular or roughly elliptical spot. For points near the center of the spot and points away from the spot by distances large compared with the radius of the spot, the exact shape of the spot will be immaterial. For an exactly circular spot the analysis can be made in polar coordinates. This analysis is discussed in a later section for completeness, but its use would require numerical work with Bessel functions, which was not considered justifiable in view of the uncertainties in the data.

Graphical Example

In order to show the nature of the heat flow in the plate, a particular case is presented in graphical form. Consider an aluminum plate with the following dimensions:

$$\text{Thickness} = b = 0.318 \text{ cm } (1/8")$$

$$\text{Source size} = \begin{cases} \alpha = 0.5 \text{ cm} \\ \beta = 0.159 \text{ cm } (1/16") \end{cases}$$

The source is then assumed to be 0.5 centimeter square and extends halfway through the plate. From the data given in the preceding section for aluminum, the temperature of the source, for a given heat input Q, is initially

$$\theta = 10.3\, Q \tag{42}$$

where Q is expressed in joules, and θ is the temperature rise above room temperature in degrees centigrade.

Temperature at point 0. - The temperature at the point 0, which is on the inside of the plate just opposite the center of the source, is considered first. Making use of equation (33) gives

$$T_0 = T_0(0,0;t)$$

$$= \theta\left|\varphi(\alpha;0,t)\right|^2 \times \psi\left(b,\frac{b}{2};0,t\right) \tag{43}$$

The function $\psi(b,b/2;0,t)$, which determines the flow of heat through the thickness of the plate, is plotted in figure 26. It starts from zero and rises to 0.5, since the flow of heat directly through the plate would double the amount of heated metal and so would lower the temperature by a factor 0.5. This function is plotted on a universal time scale as a function of t/t', where t' is defined by equation (37).

The function $\varphi(0.5;0,t)$, which determines the flow of heat away from the point 0 along the plate, is plotted in figure 27. This graph starts at unity at $t = 0$ and diminishes comparatively slowly to zero.

The composite result, giving the temperature at the point 0, is plotted as curve A in figure 28, which shows that the temperature at 0 rises to about $\theta/4$ as its maximum value in about 20 milliseconds and then falls rather steeply; in 1/10 second it is down to $\theta/10$. This point will obviously be the hottest on the inside of the plate, so that the rapidity with which it cools off will be an important criterion governing the firing of an explosive gas mixture that contacts the surface here.

Temperature at a neighboring point. - As an indication of the temperatures reached on the inside of the plate near the source point, the temperature-time curve has been plotted for a point 0.5 centimeter from the point O. The curve is given as curve B of figure 28. The temperature at this point rises slowly to only about 25 percent of the maximum temperature at O and then falls slowly. The flow of heat along the aluminum plate is so rapid that only the points quite near the initial source are heated to any great extent.

Effect of Continuous Source

It has been assumed in the previous calculations that the heat source is established instantaneously at time $t = 0$ and that only the temperature distribution from this origin is significant. In practice, the application of the heat will not be so instantaneous, but the source may be applied for some time and may vary from instant to instant in magnitude. Once the problem of finding the temperature distribution from an instantaneous source has been solved, it is possible to write the method of finding it from a variable source, taking advantage of the linearity of the differential equation of heat conduction and of the boundary conditions.

First the notation in which the result has been expressed will be revised. Instead of using the particular instant $t = 0$ as the time of application of the source, this instant is indicated as t_1. Also, suppose that the heat is supplied in an infinitesimal time interval dt_1, such that $Q = q(t_1)dt_1$. Then, from equation (31) the temperature distribution following from this source at times $t > t_1$ would be given by the formula

$$T(x,y,z,t) = \frac{q(t_1)}{c\rho\alpha^2\beta}\varphi(\alpha;x,t-t_1)\varphi(\alpha;y,t-t_1)\psi(b,\beta;z,t-t_1)dt_1 \qquad (44)$$

Clearly, to find the temperature distribution from a set of sources operating in the past it is necessary only to sum (integrate) expression (44) over all the sources that have been present. This yields the final formula:

$$T(x,y,z,t) = \frac{1}{c\rho\alpha^2\beta}\int_{-\infty}^{t} q(t_1)\varphi(\alpha;x,t-t_1)\varphi(\alpha;y,t-t_1)\psi(b,\beta;z,t-t_1)dt_1 \qquad (45)$$

It is not practicable to evaluate this expression by actual integration if the source function $q(t_1)$ is very complex. The best method

of handling it is probably by numerical and graphical means, approximating the source function by a set of discrete sources.

Treatment of Infinite Plate in Cylindrical Coordinates

The mathematical analysis of the heat flow in a plate has been carried out entirely in terms of Cartesian coordinates in the earlier sections of this report. This has led to the use of a heat source in the form of a small rectangular parallelepiped. The reader may consider that it would be more sensible to use a heat source in the form of a small cylinder. This is certainly correct in principle, and the procedure used has been one of convenience only. In this section the analysis is carried through for cylindrical polar coordinates with a cylindrical shape for the source and solved in terms of Bessel functions.

Using the usual cylindrical polar coordinates, with origin at the point O, the heat-conduction equation takes the form

$$\left[\varkappa^2\left(\frac{\partial^2}{\partial r^2}+\frac{1}{r}\frac{\partial}{\partial r}+\frac{\partial^2}{\partial z^2}\right)-\frac{\partial}{\partial t}\right]T=0 \tag{46}$$

Only cylindrically symmetric solutions need be considered, so that the temperature depends only on the distance from the center of the plate and not on the angular position around the source.

First, particular solutions of the differential equation (46) are sought which obey the boundary conditions of the problem. Here an infinitely large plate is taken at the start, so that the boundary conditions reduce to the requirement that the solution be finite everywhere, and be single-valued. There is to be no flow of heat from the surfaces of the plate, so that $\partial T/\partial z = 0$ at $z = 0,b$.

Particular solutions satisfying these conditions are of the form

$$F(r)\cos\left[\left(\frac{n\pi}{b}\right)z\right]\exp\left[-\left(\frac{n\pi\varkappa}{b}\right)^2 t\right]\exp\left(-\lambda^2 t\right) \tag{47}$$

where λ is an arbitrary real positive constant, and $F(r)$ is a solution of the differential equation

$$\left(\frac{d^2}{dr^2}+\frac{1}{r}\frac{d}{dr}+\lambda^2\right)F(r)=0 \tag{48}$$

The only solution of equation (48) that remains finite at $r = 0$ (for $\lambda \neq 0$) is

$$F(r) = \text{constant} \times J_0(\lambda r) \tag{49}$$

where J_0 is the Bessel function of first kind of order zero.

To satisfy the initial conditions these particular solutions are combined linearly. The members in the variable z must be summed over the non-negative integer $n = 0,1,2 \ldots$, while the radial solutions must be integrated over the parameter λ. If the initial heat source is a small cylinder of radius a and depth β, into which an amount of heat Q is deposited at $t = 0$, the result is

$$T(r,z,t) = \frac{Q}{c\rho\pi a^2 \beta} \varphi(a;r,t)\psi(b,\beta;z,t) \tag{50}$$

with

$$\psi(b,\beta;z,t) = \frac{\beta}{b} \sum_{m=0}^{\infty} \frac{(-)^n \cos\left[\left(\frac{n\pi}{b}\right) z\right]}{\frac{1}{2}(1 + \delta_{n,0})} \frac{\sin\left(\frac{n\pi\beta}{b}\right)}{\frac{n\pi\beta}{b}} \exp\left[-\left(\frac{n\pi\alpha}{b}\right)^2 t\right] \tag{51}$$

which is identical with the function defined in equation (20). The function $\varphi(a;r,t)$ is of the form

$$\varphi(a;r,t) = \int_0^{\infty} g(\lambda)\ J_0(\lambda r)\ \exp(-\lambda^2 t)\lambda\ d\lambda \tag{52}$$

where $g(\lambda)$ must be determined from the initial conditions. Here the following is required:

$$\varphi(a;r,0) = \begin{cases} 0 & \text{if } r > a \\ 1 & \text{if } r < a \end{cases} \tag{53}$$

If

$$\varphi(a;r,0) = u(r) \tag{54}$$

Then, from equation (52),

$$u(r) = \int_0^{\infty} g(\lambda)\ J_0(\lambda r)\lambda\ d\lambda \tag{55}$$

The inversion of this integral equation for $g(\lambda)$ when the left side is a known function gives

$$g(\lambda) = \int_0^\infty u(r)\ J_0(\lambda r) r\ dr \tag{56}$$

Making use of the initial conditions (53) which define the function $u(r)$, in the present problem

$$g(\lambda) = \int_0^a J_0(\lambda r) r\ dr \tag{57}$$

This leads to the formula

$$\varphi(a;r,t) = \int_0^\infty \left[\int_0^a J_0(\lambda R) R\ dR \right] J_0(\lambda r)\ \exp(-\lambda^2 t)\lambda\ d\lambda$$

$$= \int_0^a \left[\int_0^\infty J_0(\lambda R)\ J_0(\lambda r)\ \exp(-\lambda^2 t)\lambda\ d\lambda \right] R\ dR \tag{58}$$

It would be possible to make use of these formulas for the calculation of the temperature distribution in the plate, but the work would be greater than by the earlier method, without significant increase in accuracy of the result.

REFERENCES

1. Stout, H. P., and Jones, E.: The Ignition of Gaseous Explosive Media by Hot Wires. Third Symposium on Combustion and Flame Phenomena, The Williams & Wilkins Co., 1949, pp. 329-336.

2. Peirce, B. O.: A Short Table of Integrals. Third ed., Ginn and Company, 1929.

TABLE I. - COMPARISON OF PEAK CURRENT, MECHANICAL FORCES, HEATING EFFECT, AND CHARGE TRANSFER OF THREE TYPES OF SURGE CURRENT GENERATORS THAT REPRODUCE EFFECTS OF NATURAL LIGHTNING ON AIRCRAFT

	High-current generator, 3.3 μf at 150 kv	Secondary stroke generator, 3,000 μf at 10 kv	Long-duration current generator, 200 amp at 12 kv
Peak current, duration and wave form	100,000-amp duration = 10^{-5} sec to 1/2 value critically damped	5,000-amp duration = 10^{-2} sec to 1/2 value critically damped	200-amp duration = 1 sec rectangular wave
Relative mechanical force, proportional to square of peak current ($amp^2 \times 10^{-8}$)	100.0	0.25	0.0004
Relative heating effect, proportional to energy released $\left(R\int_0^\infty I^2\,dt, \text{ joules}\right)$	= 69,000 R	= 172,000 R	= 40,000 R
Relative erosion and pitting effect, proportional to charge transfer	(C)×(E) $3.3\times10^{-6} \times 15\times10^{4}$ = 0.5 coulomb	(C)×(E) $3{,}000\times10^{-6} \times 10{,}000$ = 30 coulombs	(I)×(t) 200 × 1 = 200 coulombs

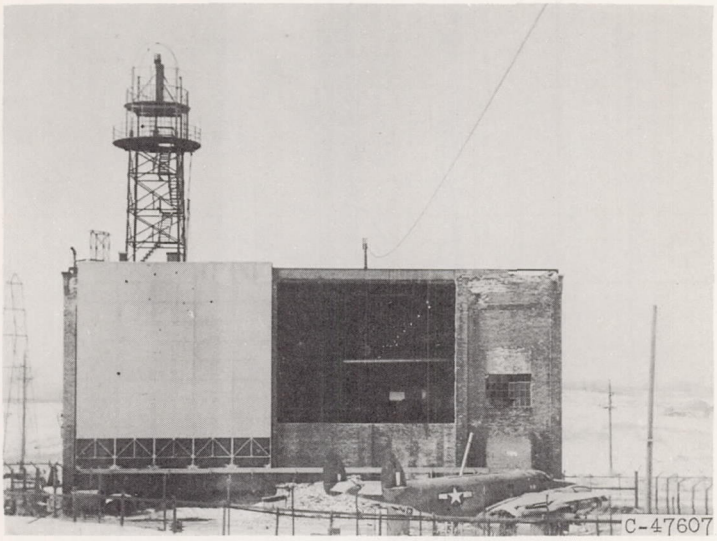

(a) Laboratory building and network.

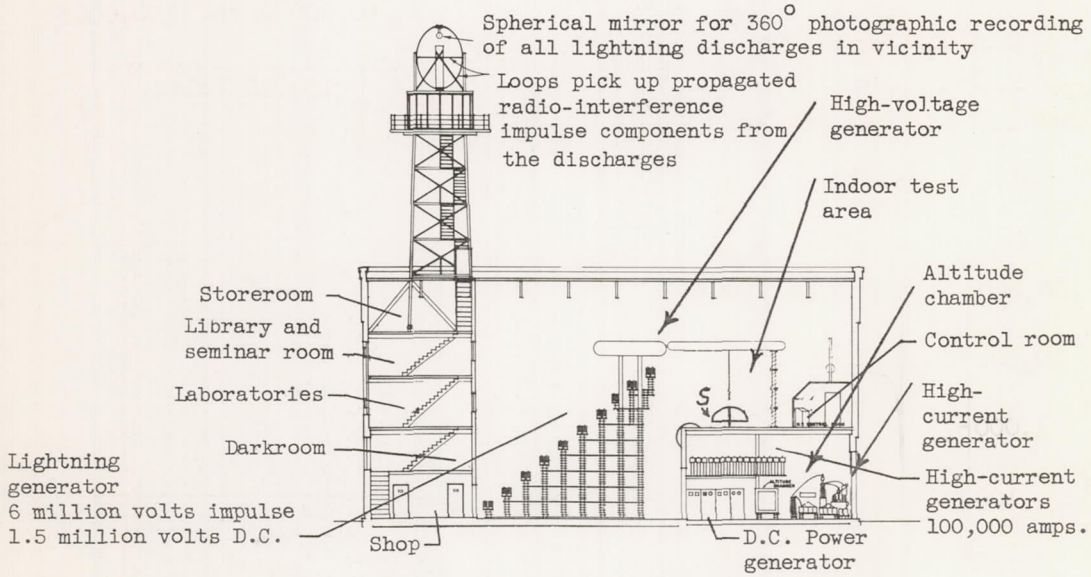

(b) Cross section of laboratory showing test facilities.

Figure 1. - Lightning and Transients Research Institute laboratory for producing simulated lightning channel.

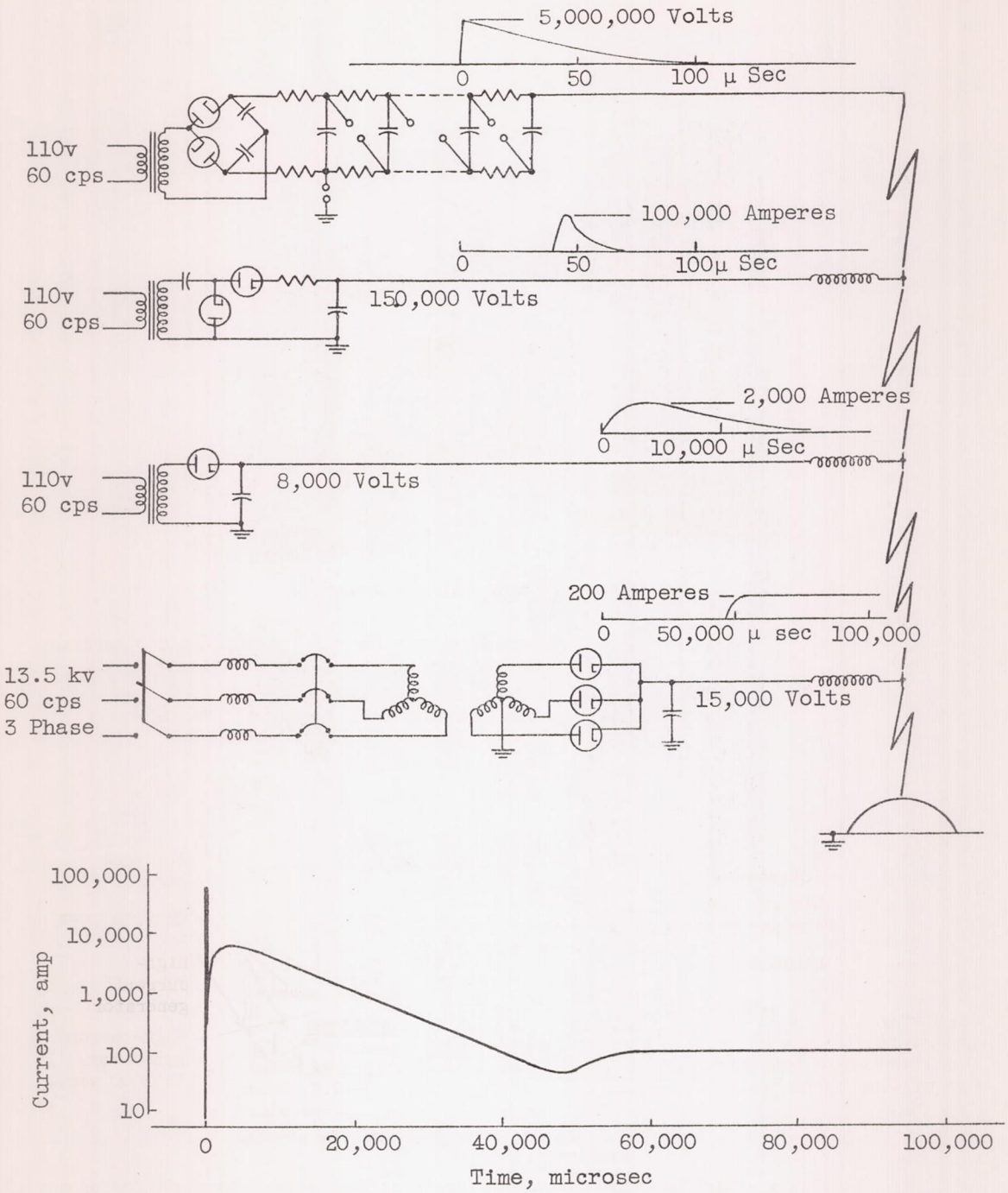

Figure 2. - Composite waveform generators and resulting waveform.

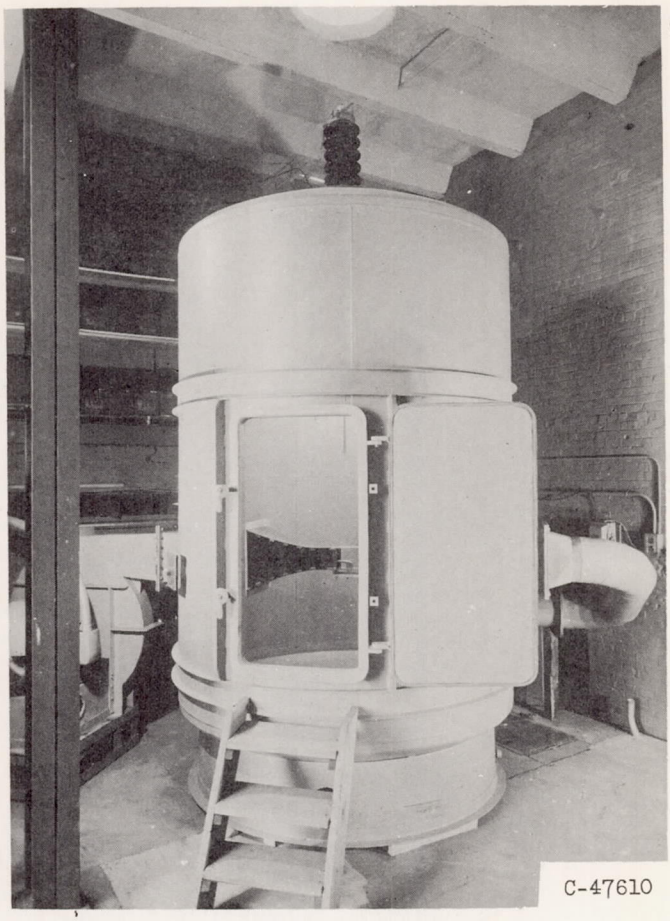

Figure 3. - Environmental explosion chamber with integral wind tunnel.

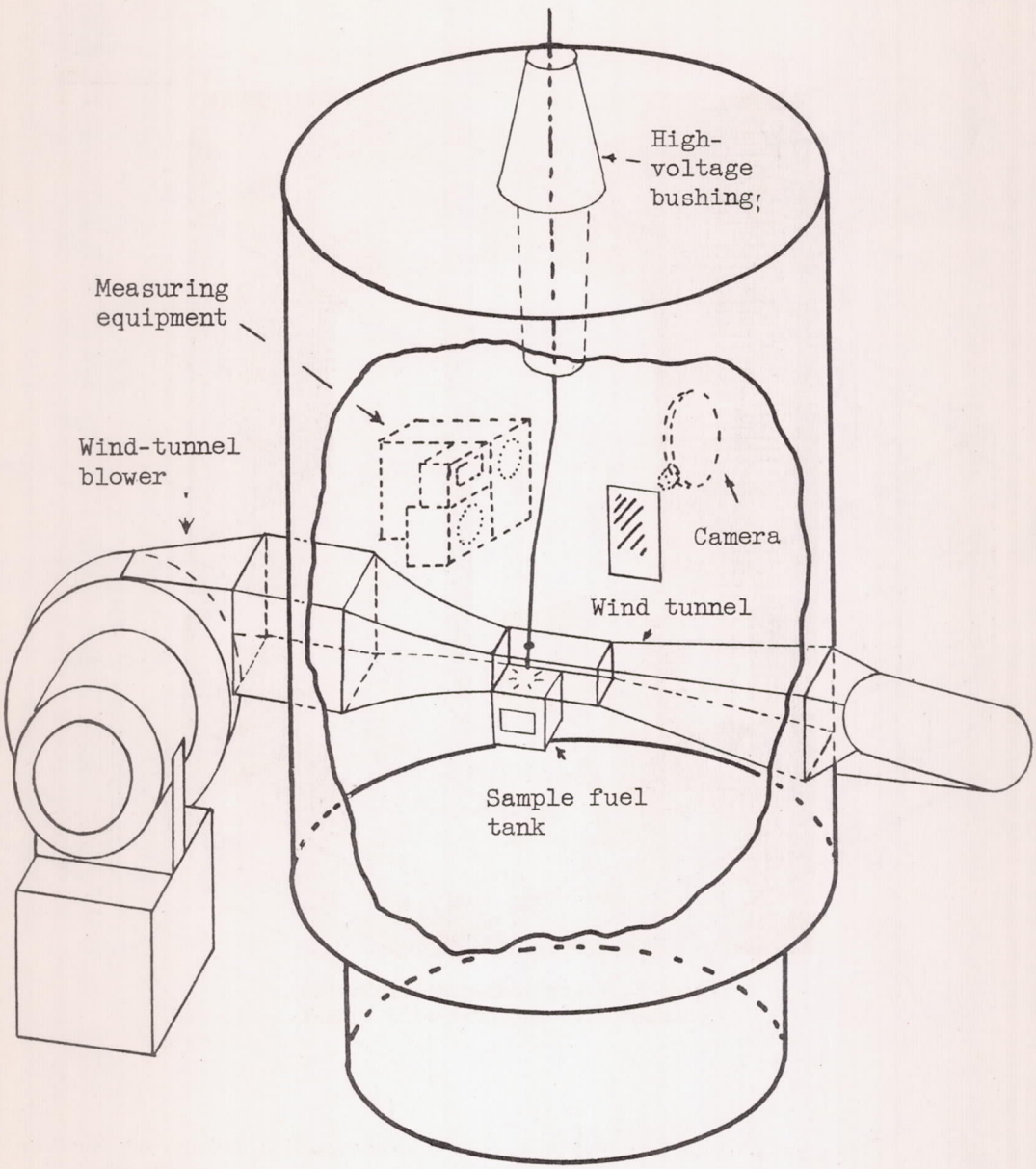

Figure 4. - Schematic diagram of environmental explosion chamber showing location of integral wind tunnel, camera, and measuring equipment.

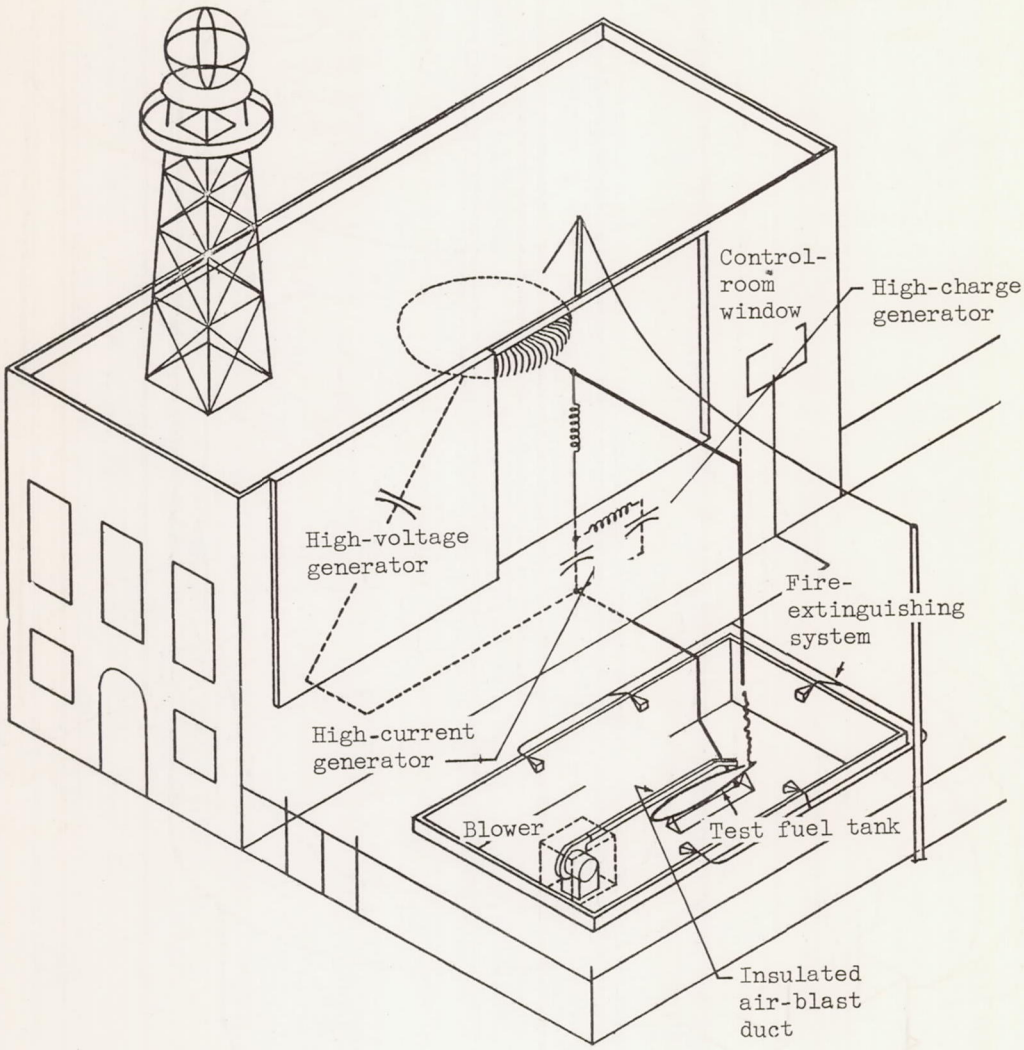

Figure 5. - Concrete-block pit for full-scale experimental setups to control possible explosion and fire hazards from ignited fuels during laboratory tests involving discharges to full-size fuel tanks.

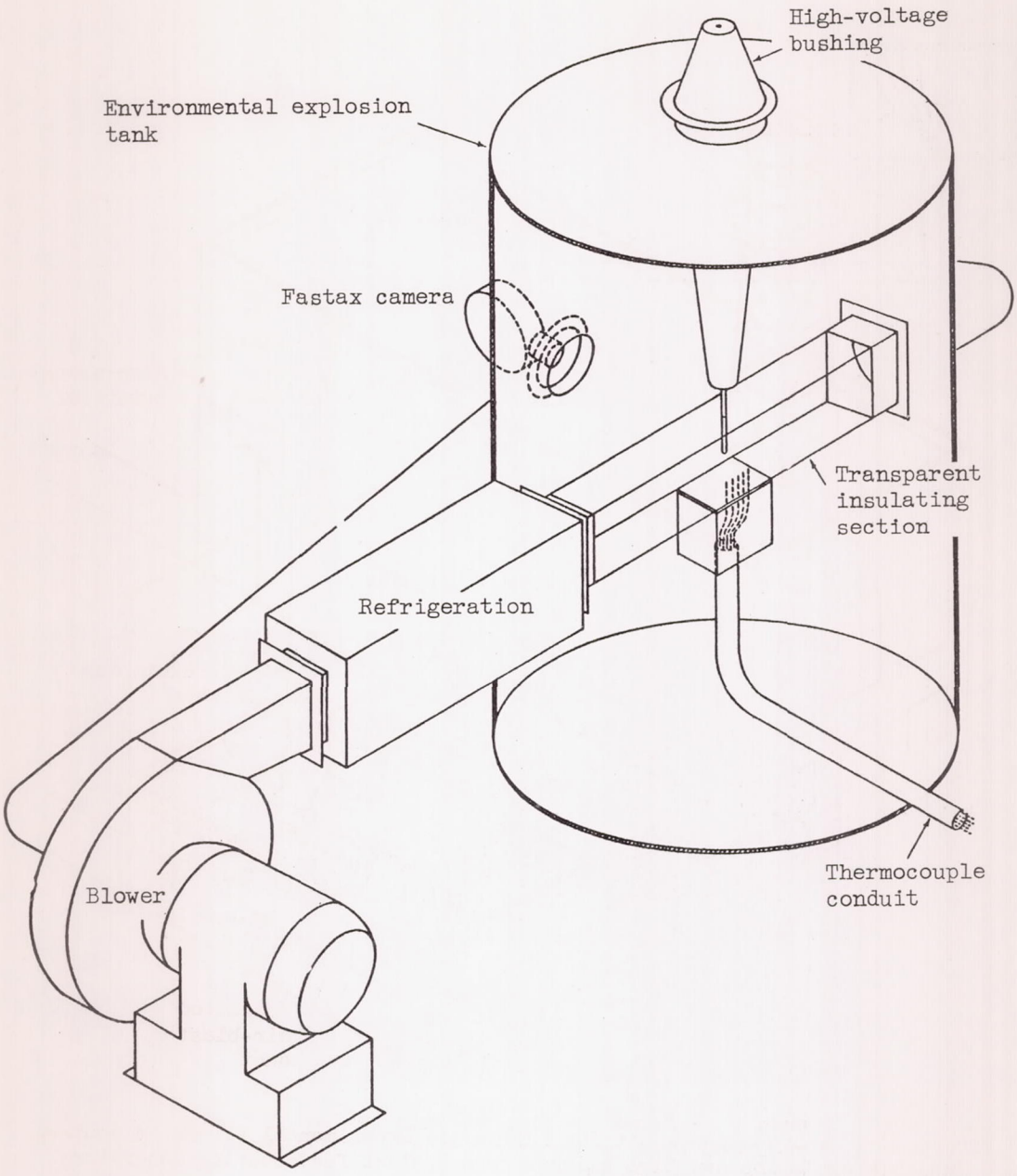

Figure 6. - Environmental explosion tank for test setups with discharge to small fuel cells under different conditions of temperature, air velocity, and pressure.

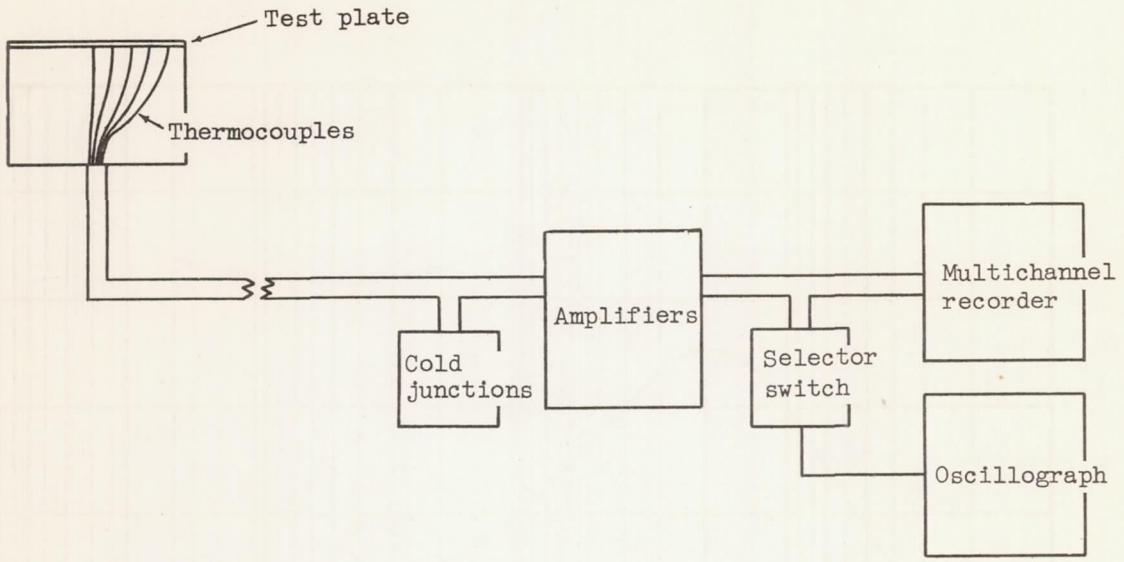

Figure 7. - Block diagram of thermocouple system.

Figure 8. - Cross section through center of crater produced by laboratory discharge to 1/8-inch-thick aluminum plate.

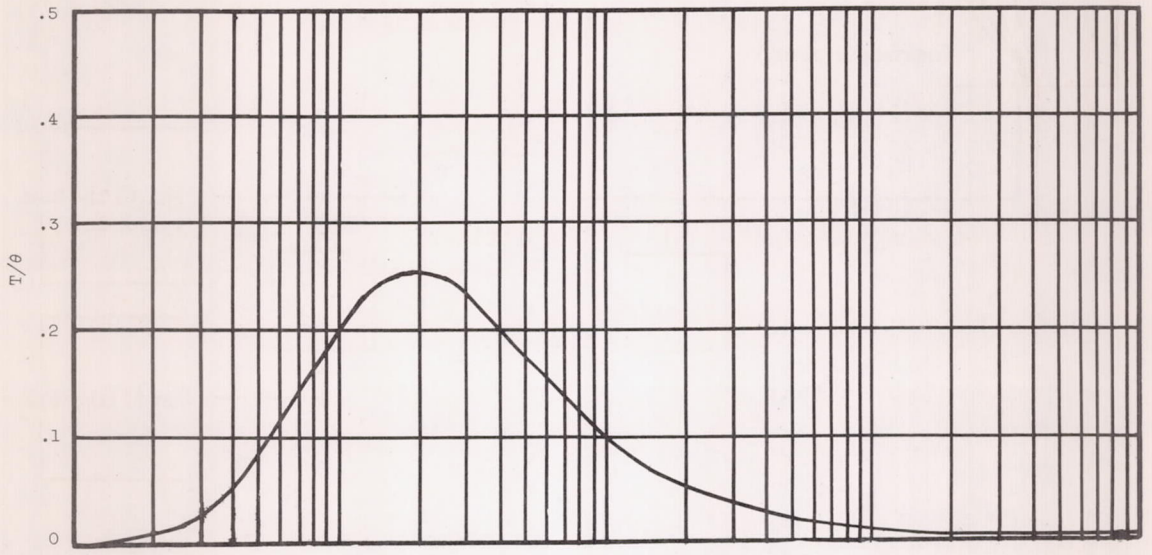

(a) Theoretical curve.

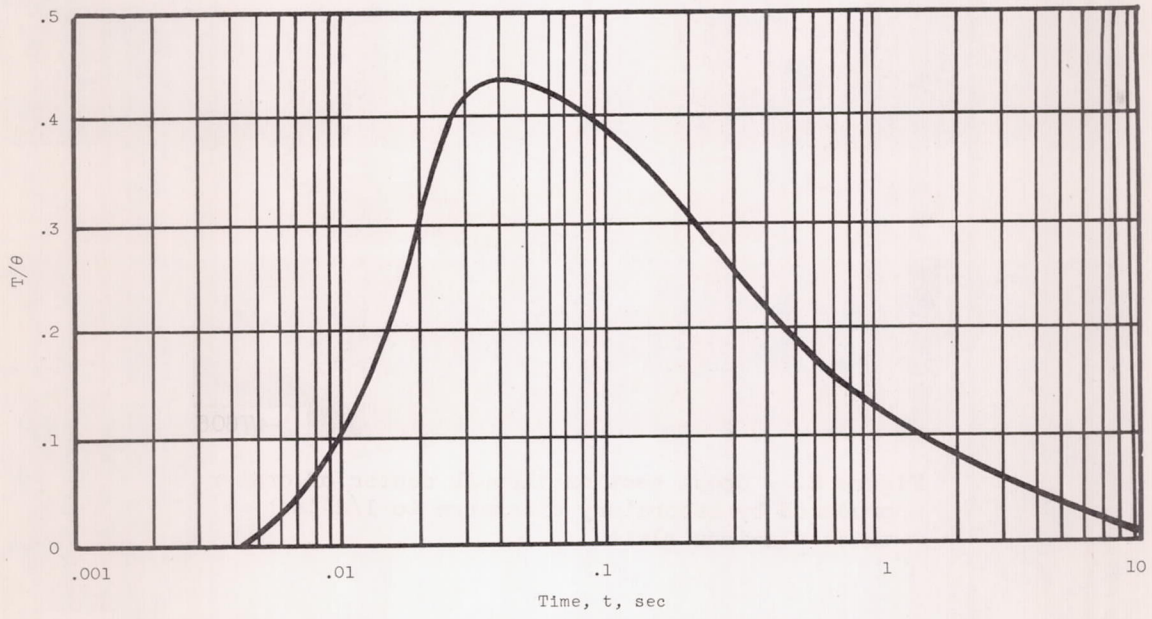

(b) Experimental curve.

Figure 9. - Temperature-time curves for 1/8-inch-thick aluminum plate.

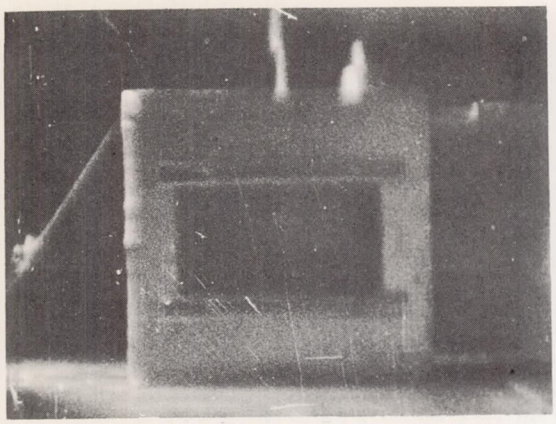

0 Sec

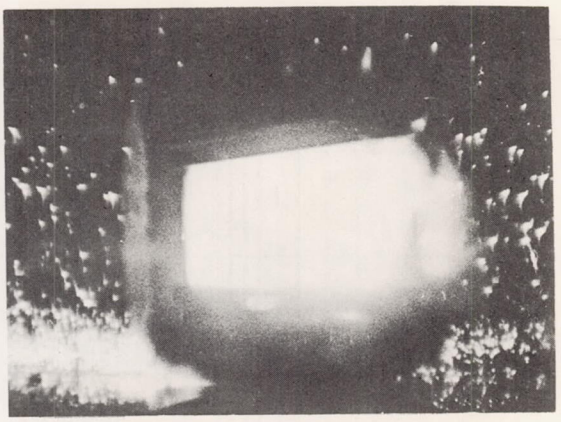

0.038 Sec

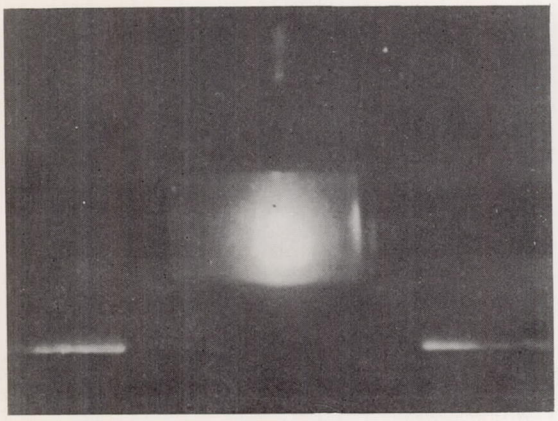

0.004 Sec

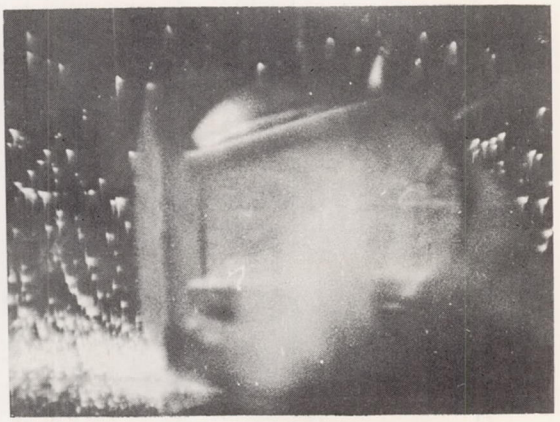

0.040 Sec

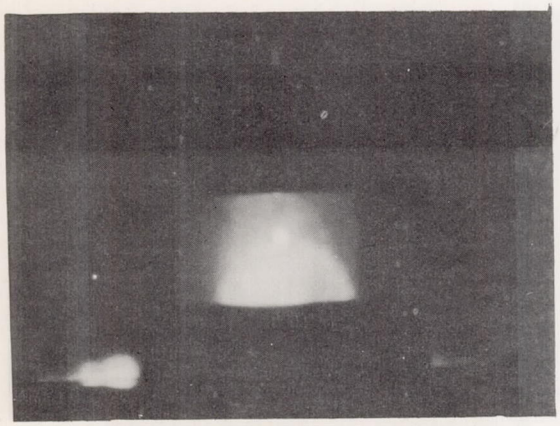

0.010 Sec

C-47616

0.204 Sec

Figure 10. - Photographic sequence of sample fuel-tank ignition by artificial-lightning discharge.

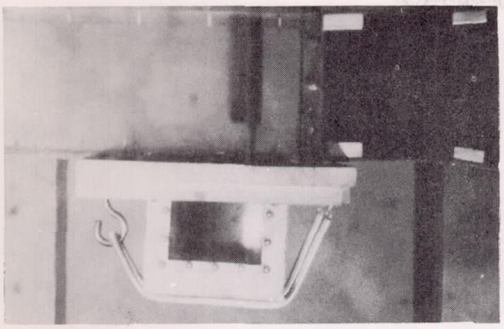

0 Sec

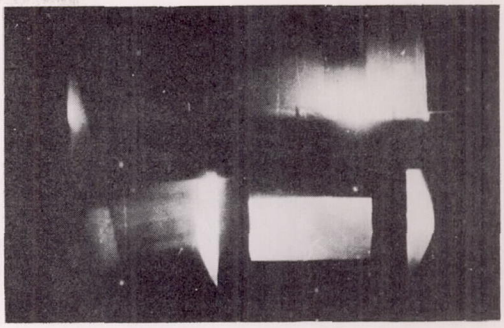

0.061 Sec

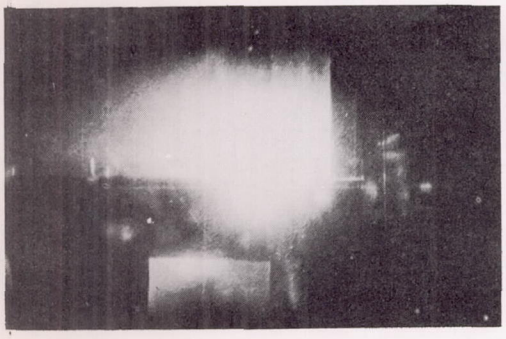

0.055 Sec

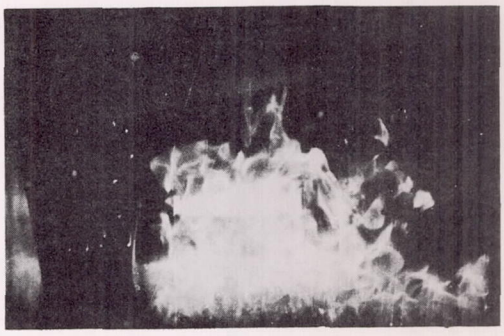

0.081 Sec

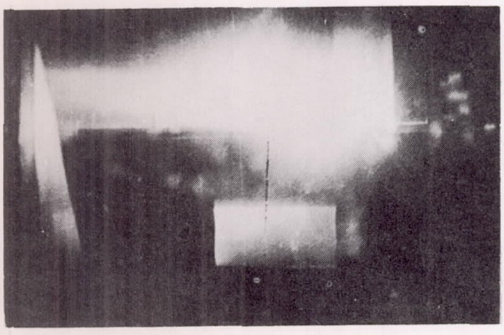

0.058 Sec

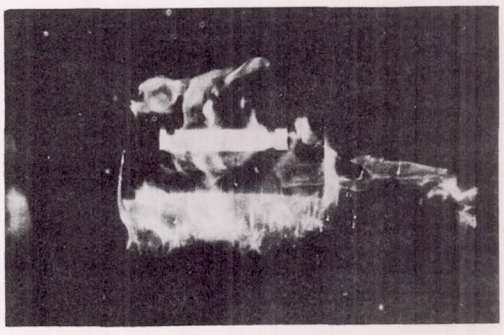

0.110 Sec

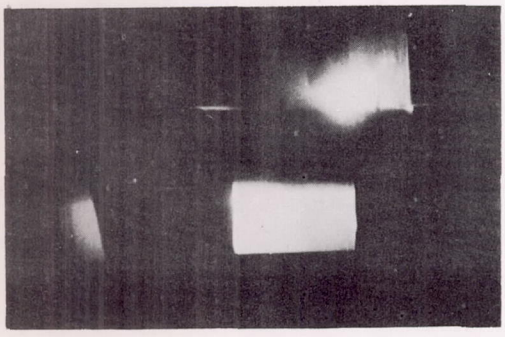

0.060 Sec

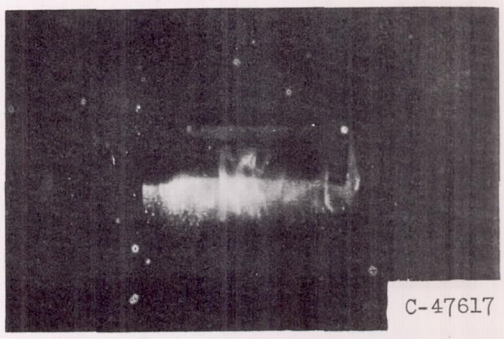

0.120 Sec

Figure 11. - Fuel-tank explosion by artificial-lightning discharge with 300-mph windstream.

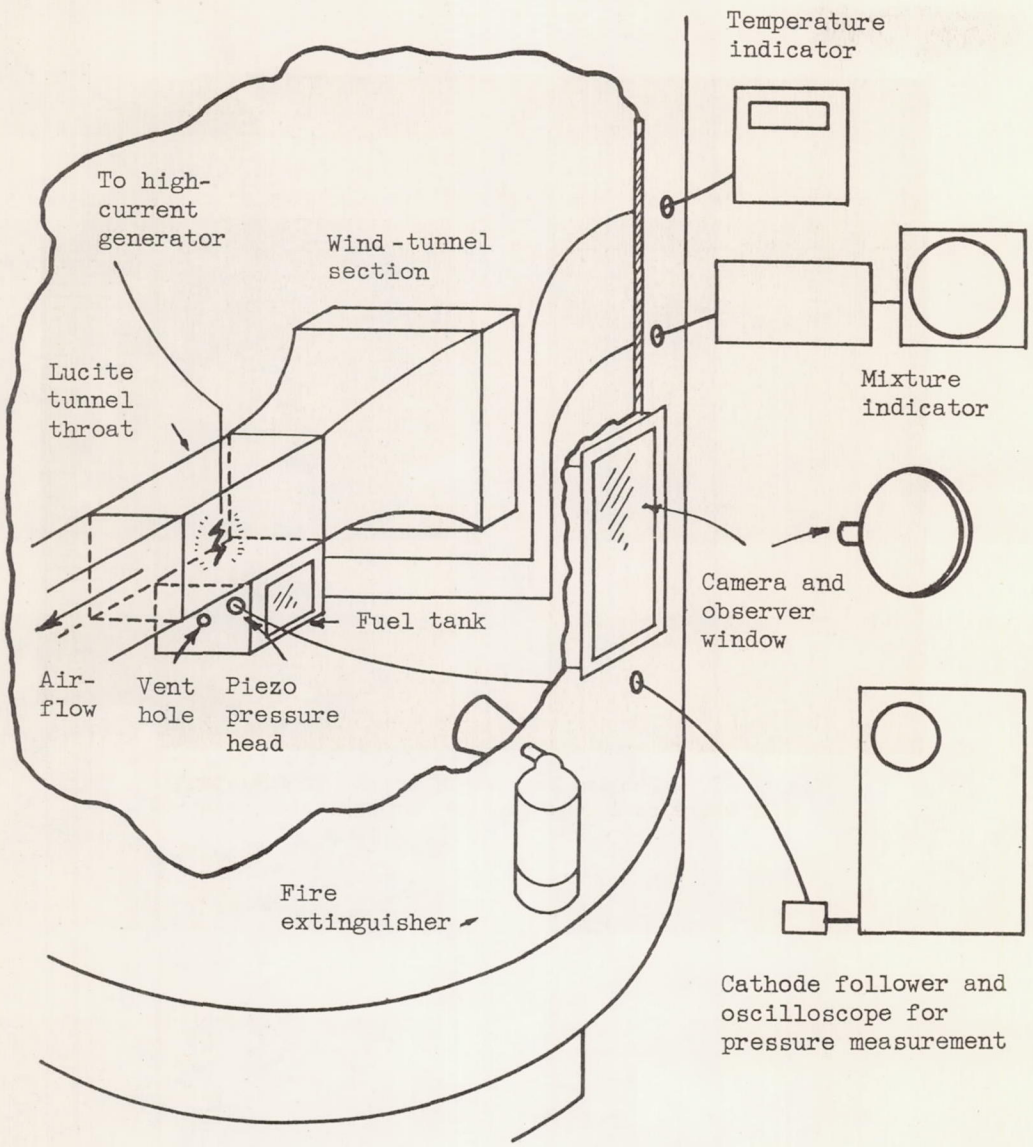

Figure 12. - Test arrangement for scale fuel-tank explosion studies.

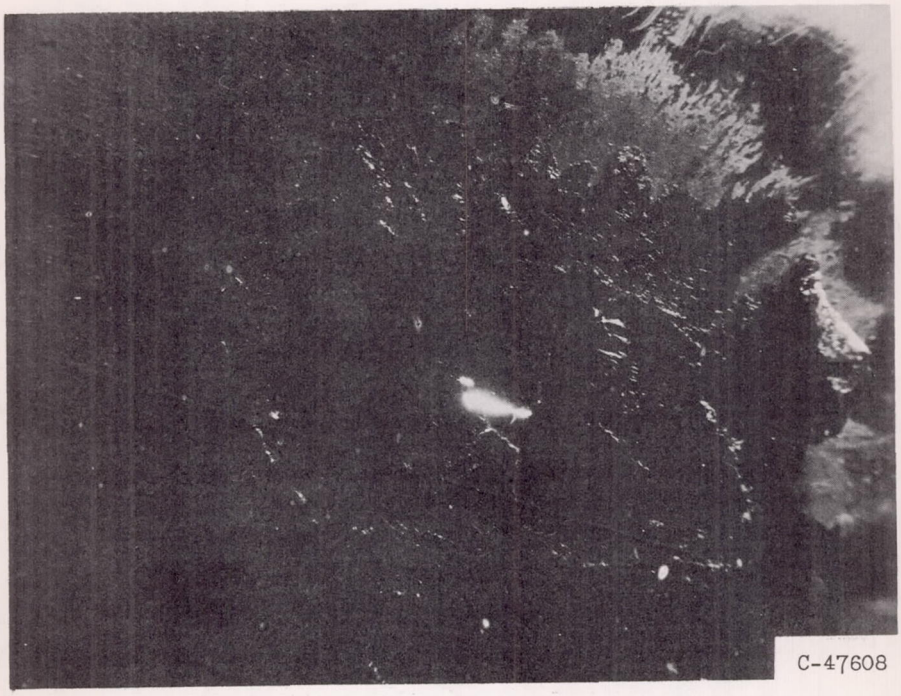

Figure 13. - Photomicrograph of cracks in fuel-tank wall where no direct puncture or explosion occurred.

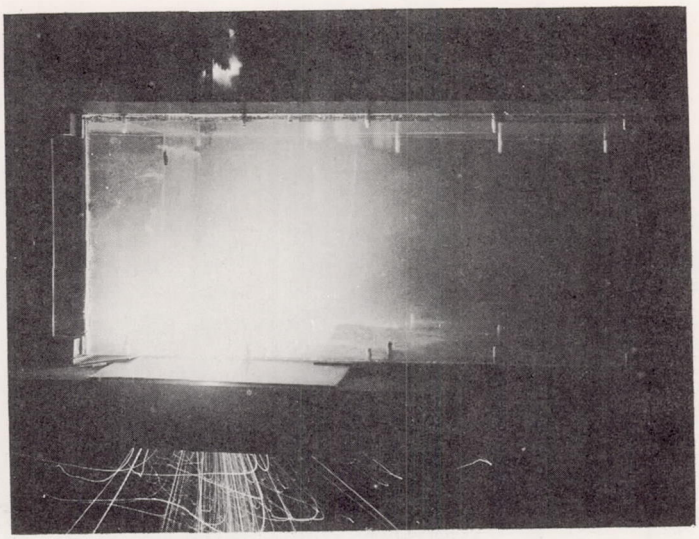

(a) Without windstream.

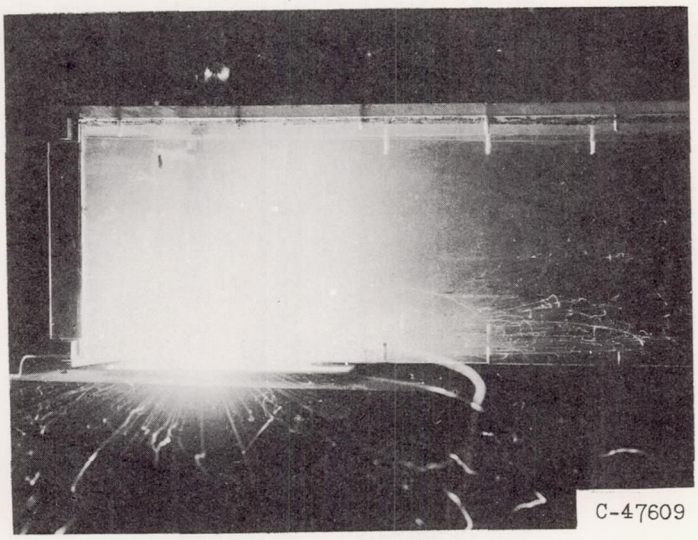

(b) With windstream.

Figure 14. - Spark showers from punctured aluminum sheet with and without windstream.

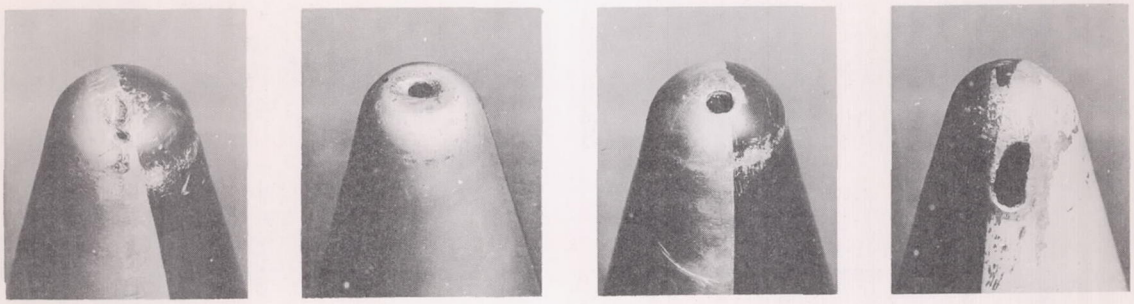

(a) Holes burned in ends of wingtip tank cones by natural lightning.

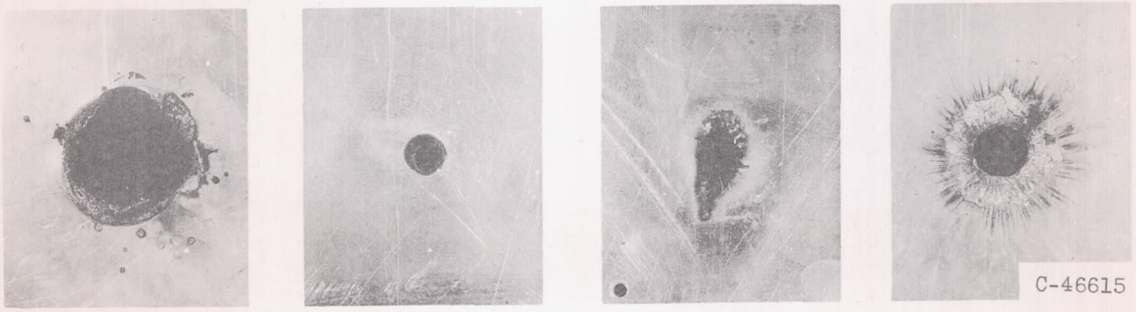

200-coulomb long-duration 200-amp peak

30-coulomb long-duration 500-amp peak

30-coulomb long-duration 4000-amp peak

30 coulombs with short pulse 150,000 amp

(b) Holes burned in 20-mil aluminum by laboratory-generated artificial discharges.

Figure 15. - Comparison of holes burned by natural and artificial lightning.

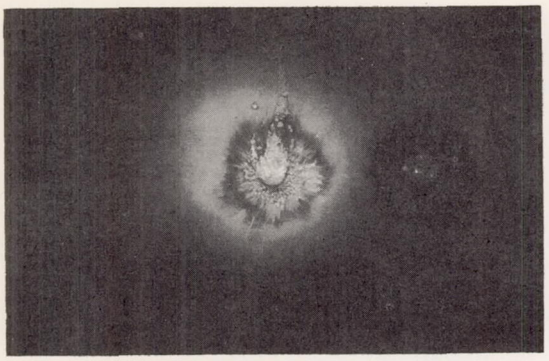

(a) Puncture of 0.064-inch sheet by standard 230-coulomb discharge.

(b) Erosion but no puncture in 0.081-inch sheet by standard discharge.

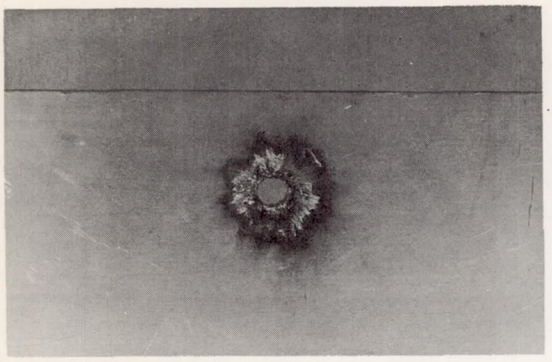

(c) Puncture of double-wall 0.040-inch sheet spaced 1/8 inch.

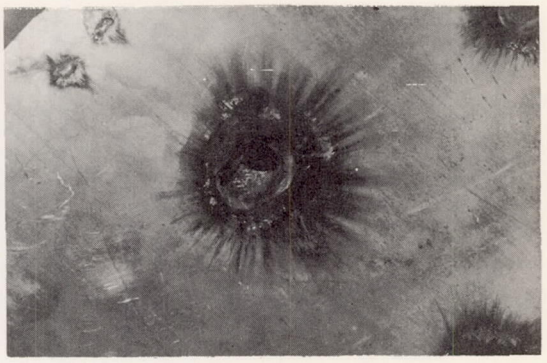

(d) Puncture of 0.040-inch sheet by 20-coulomb discharge.

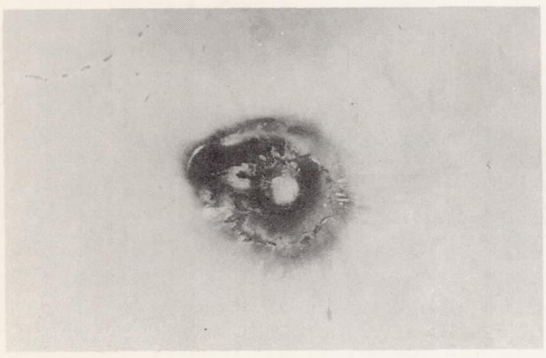

(e) Puncture of 0.081-inch sheet with windstream and faulty discharge.

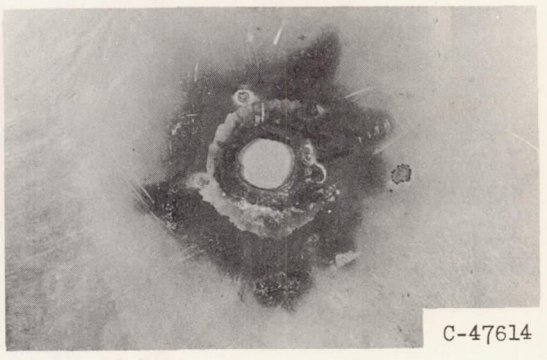

(f) Erosion of 0.081-inch sheet with windstream and standard discharge.

Figure 16. - Erosion or puncture of fuel-tank aluminum alloys (shown half size) by artificial-lightning discharges.

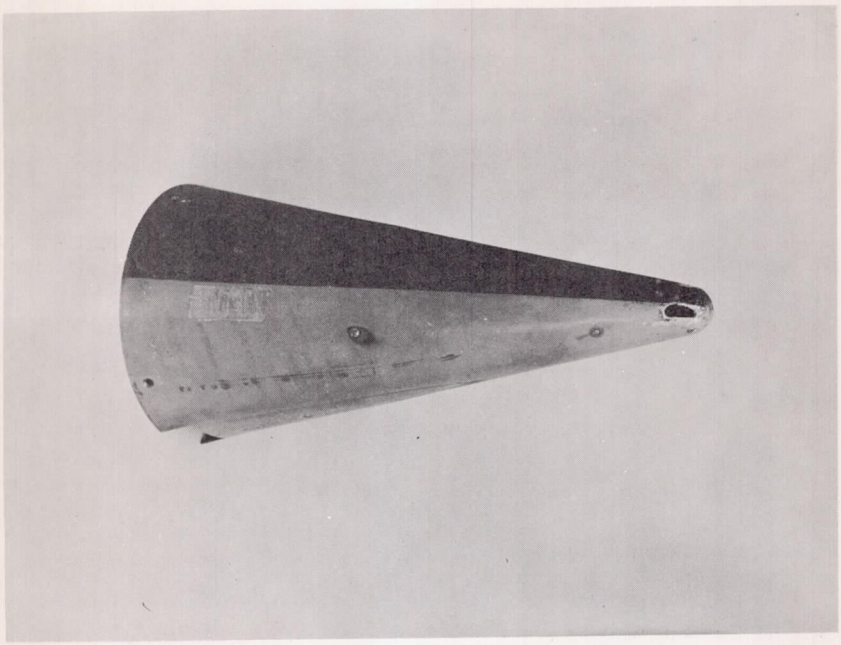

Figure 17. - Hole and pit marks on a wingtip fuel-tank tailcone caused by natural lightning.

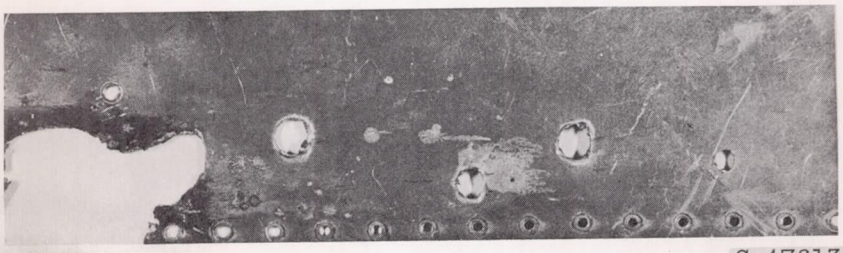

C-47613

Figure 18. - Successive in-line displacements of holes burned by natural lightning in 20-mil aluminum aircraft skin as aircraft moved through discharge.

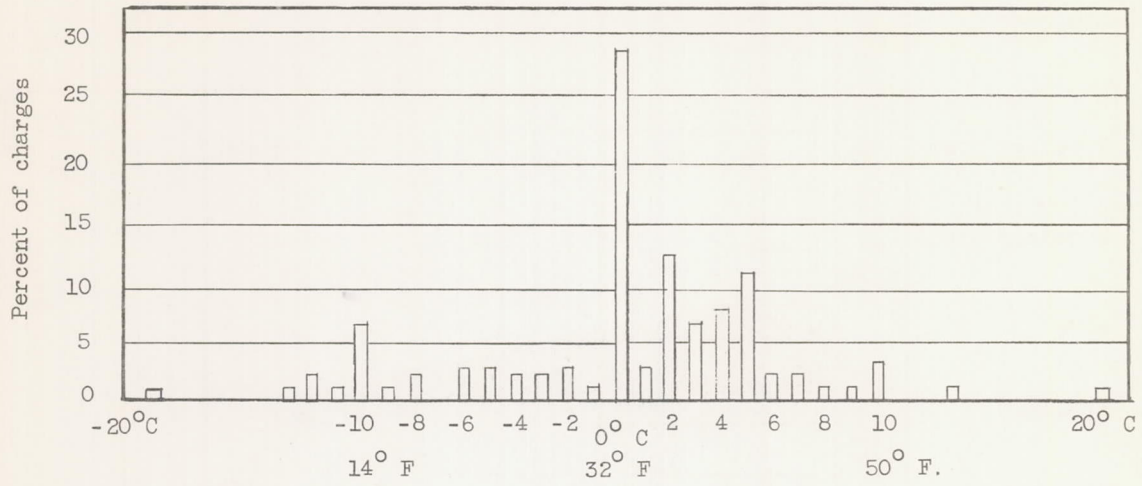

Figure 19. - Variation of percentage of lightning strokes to aircraft with temperature in U.S. flights.

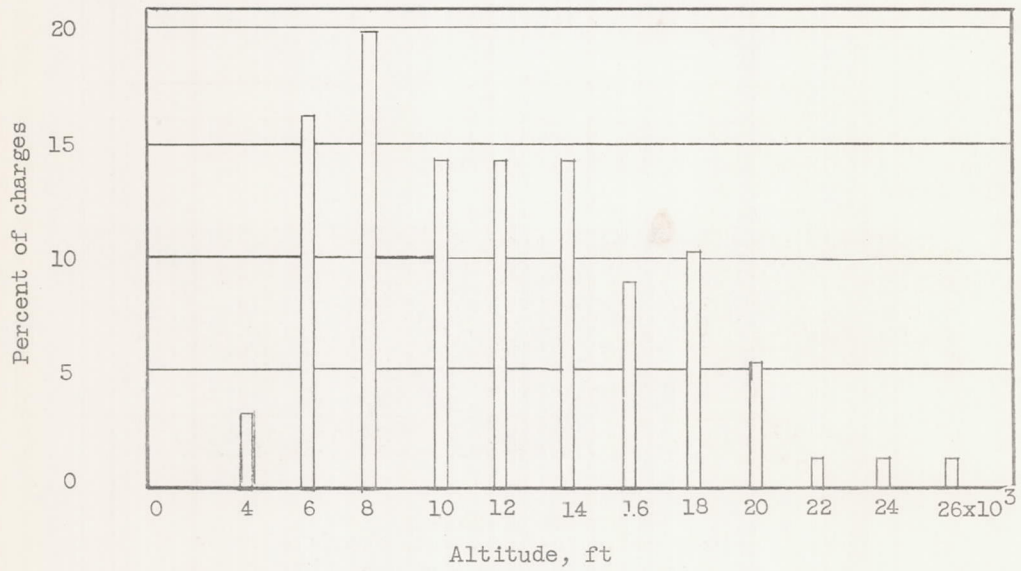

Figure 20. - Variation of lightning strokes to aircraft with altitude in U.S. flights; 123 incidents.

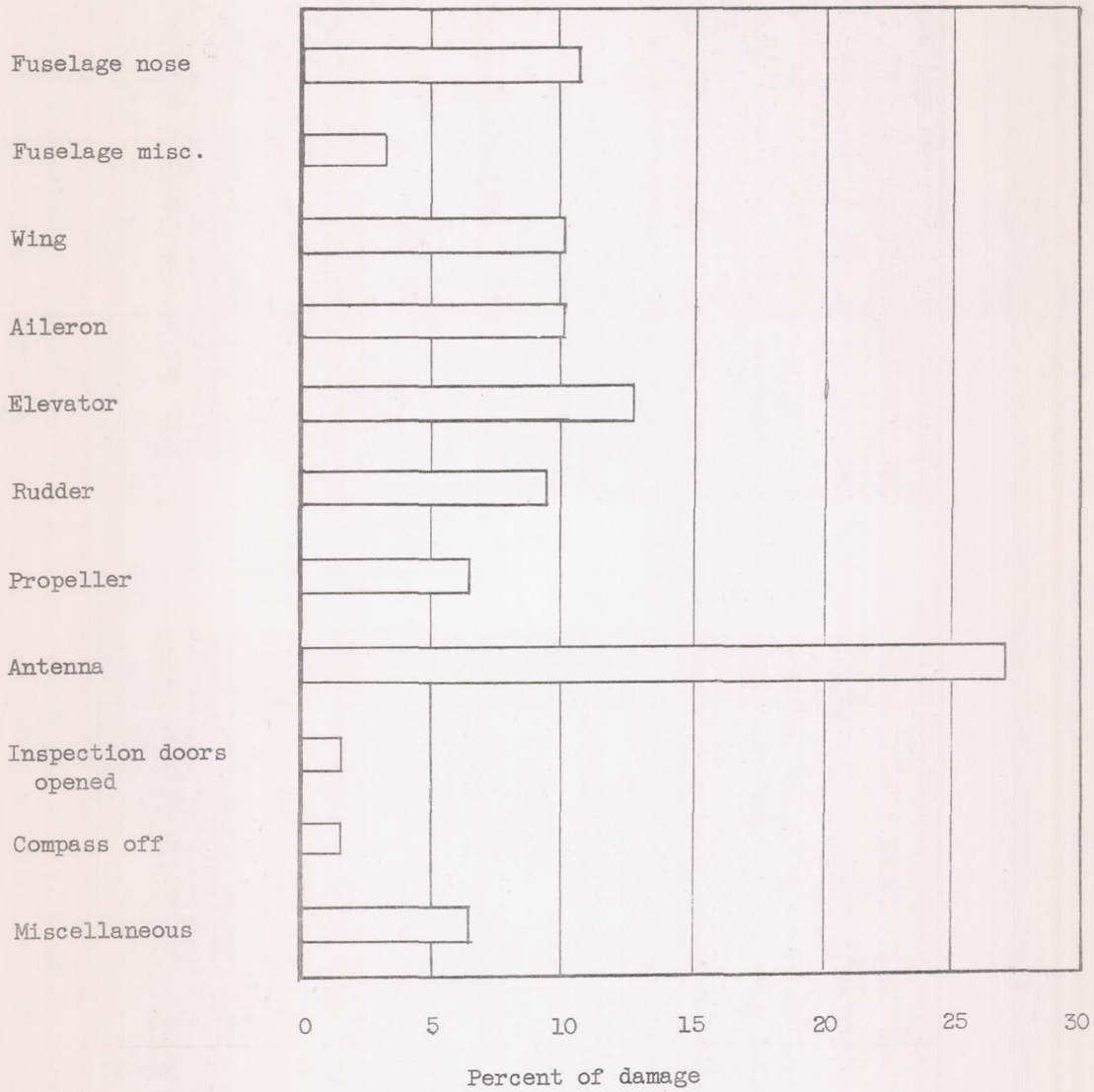

Figure 21. - Distribution of damage in 275 lightning discharges to aircraft.

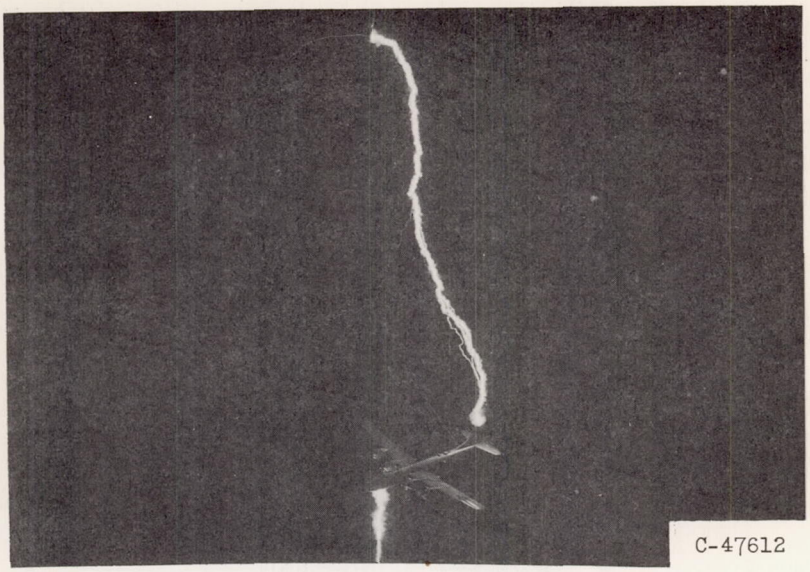

Figure 22. - Two-million-volt discharge entering model aircraft vertical fin and leaving antenna mast below fuselage.

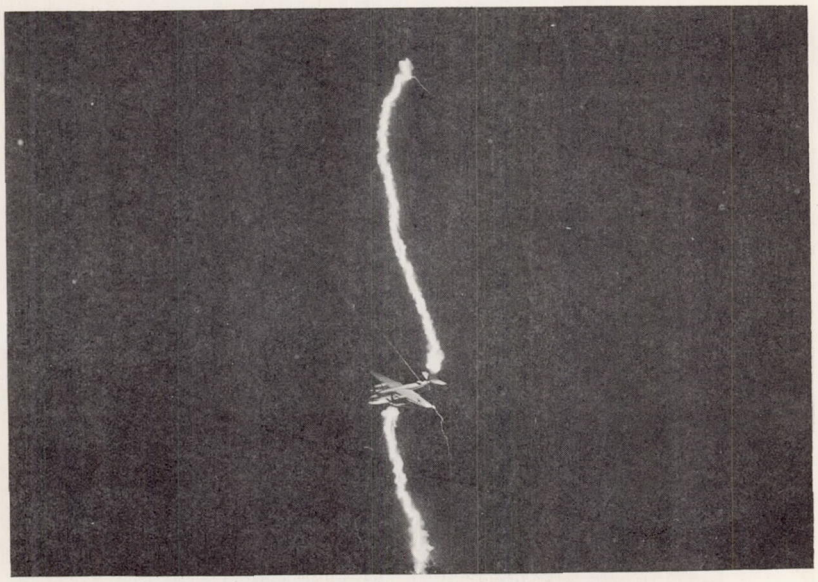

Figure 23. - Two-million-volt discharge entering model aircraft vertical fin and leaving propeller. A streamer may be noted off wingtip.

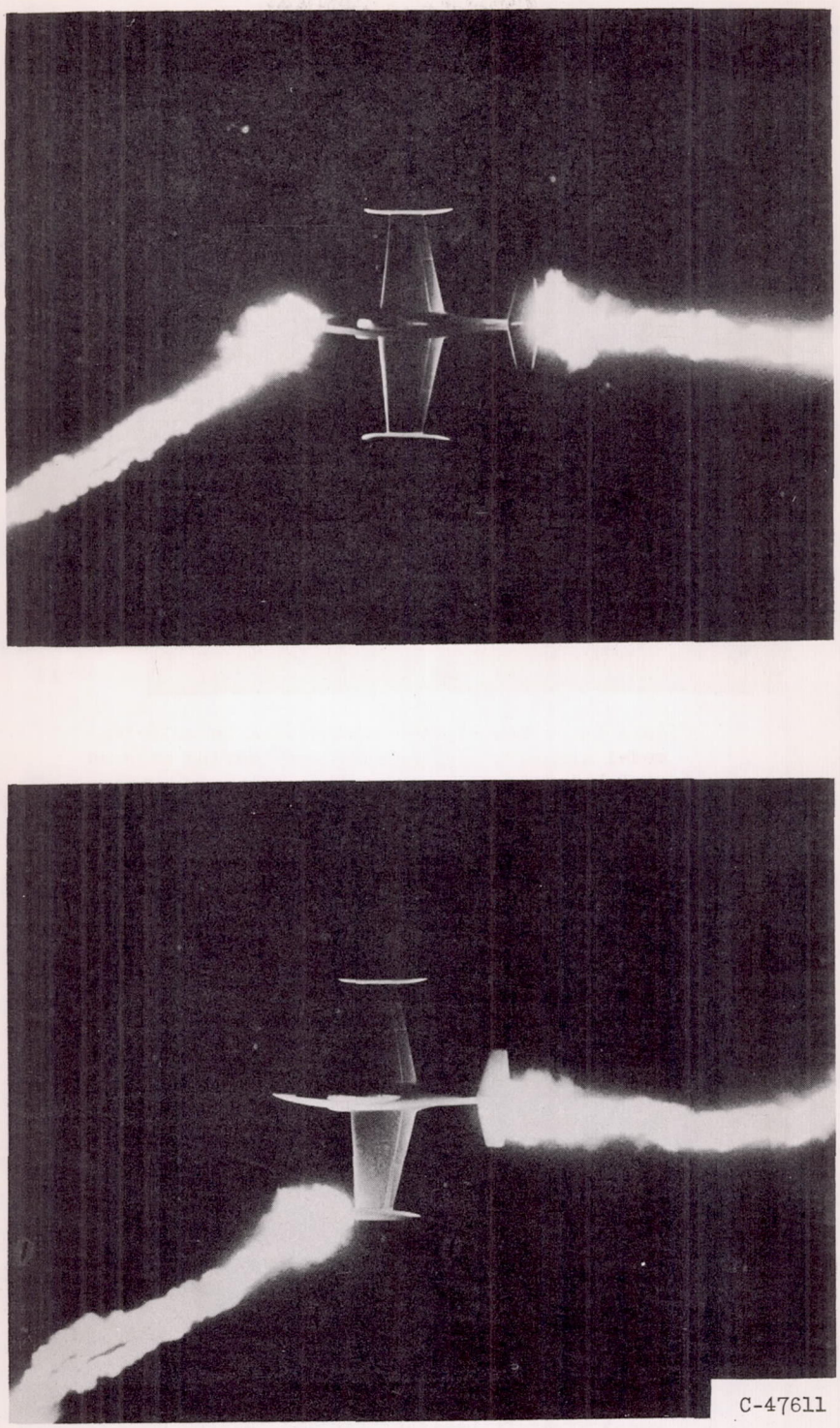

Figure 24. - Laboratory discharges to scale model of jet aircraft showing strokes to nose and wingtip tank.

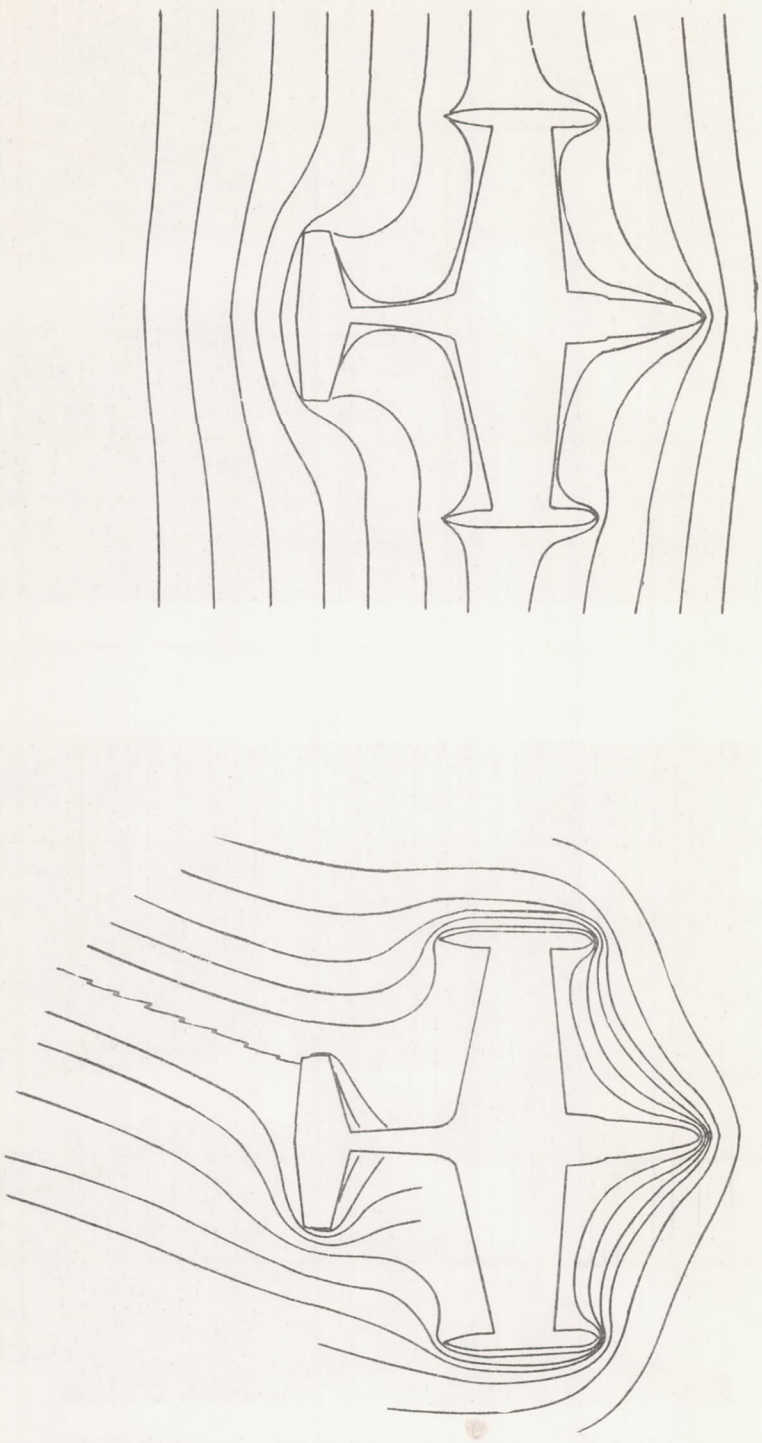

Figure 25. - Plot of equipotentials about jet aircraft in cross field before and after lightning stroke contacts tail of aircraft.

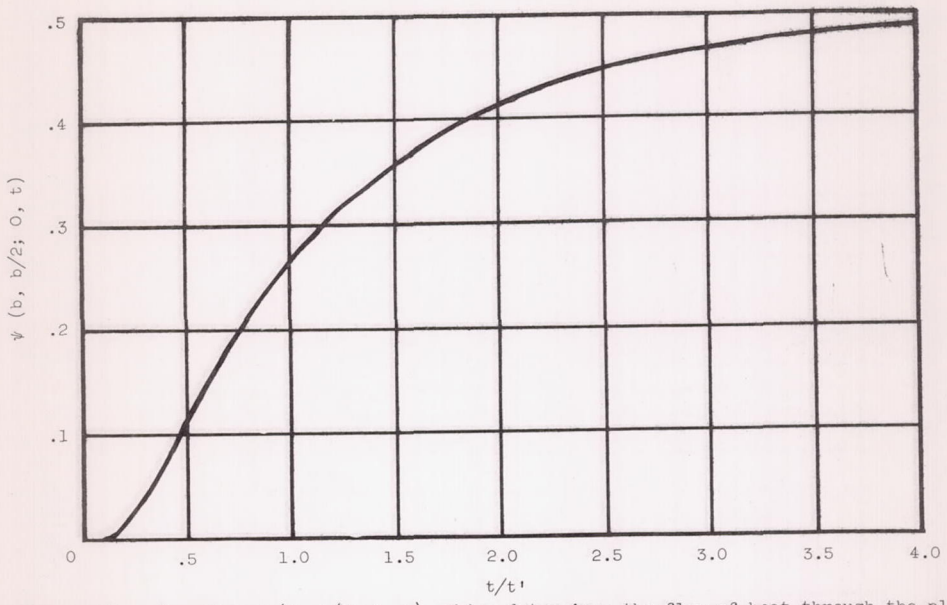

Figure 26. - Function ψ (b, b/2; 0, t). which determines the flow of heat through the plate.

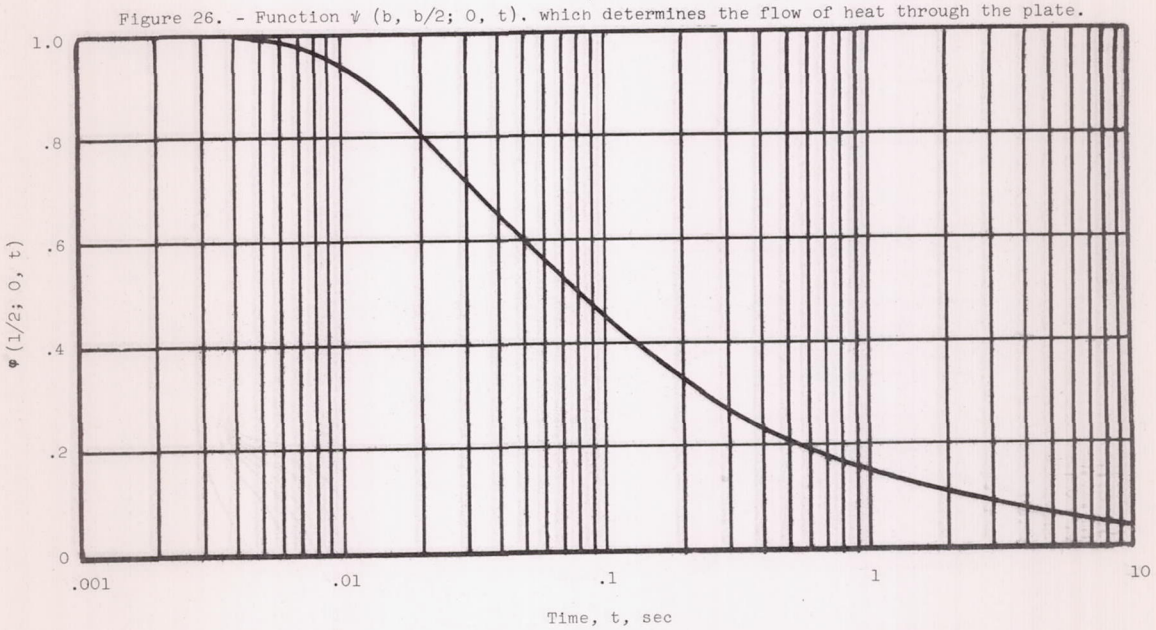

Figure 27. - Function Φ (1/2; 0, t), which determines the flow of heat along the plate.

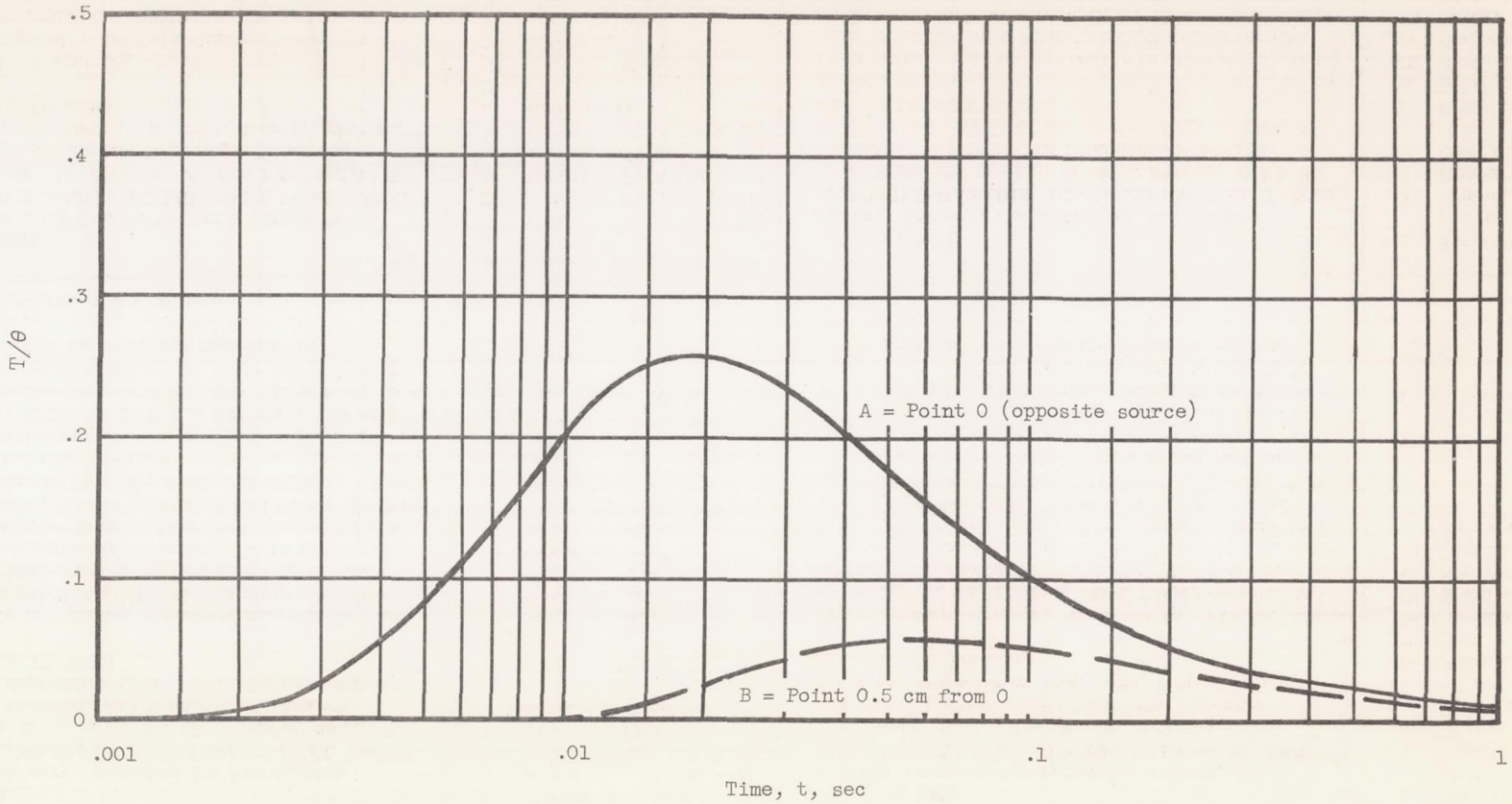

Figure 28. - Temperature-time curves; b = 0.318 centimeter (1/8 in.); β = 0.159 centimeter (1/16 in.); and α = 0.5 centimeter.

NACA - Langley Field, Va.